Long-term adaptation to hypoxia provides insight into mechanisms facilitating the switch of *Pseudomonas aeruginosa* to chronic lung infections

Joanna Drabinska[1,2]*, Lucia O'Connor[1,2], Niamh Duggan[1,2], Ciarán J. Carey[1,2], Siobhán McClean[1,2]*

[1]School of Biomolecular and Biomedical Sciences, University College Dublin, Belfield, Dublin, Ireland.

[2]Conway Institute of Biomolecular and Biomedical Science, University College Dublin, Belfield, Dublin, Ireland.

*Corresponding authors

Email: siobhan.mcclean@ucd.ie; joanna.drabinska@ucd.ie

Abstract

Opportunistic bacterial infections are an increasing threat, especially for immunocompromised individuals such as people with cystic fibrosis (CF), driving morbidity and mortality. *Pseudomonas aeruginosa* is a key pathogen associated with chronic lung infections, that has been extensively studied in this context, but the mechanism(s) driving its adaptation towards chronic colonisation in the lung are not fully understood. This work focuses on the adaptations of *P. aeruginosa* to long-term hypoxia, one of the important environmental pressures present in the CF lung, to investigate whether it drives the development of persistence in CF patients. We used an experimental evolution approach to investigate how an early CF strain adapted to 6% oxygen over 28 days. We focussed on the impact of long-term hypoxia on the proteome and investigated the emergence of stable changes in phenotype. Changes in the abundance of >140 proteins were observed compared to the ancestral strain, including proteins involved in antibiotic resistance, stress response, iron homeostasis, biofilm formation and those previously associated with chronic infection. Significant changes in the abundance of proteins regulating cellular c-di-GMP levels were also observed. We show that two distinct *P. aeruginosa* small colony variants (SCVs) emerged, one exclusively in hypoxia exposed cultures. Hypoxia-adapted cultures developed resistance to 8 out of 13 antibiotics tested; increased biofilm and exopolysaccharide production; and decreased pyocyanin production, consistent with the changes in the proteome. All hypoxia-adapted cultures showed decreased siderophore production. Overall, we demonstrate that long-term hypoxia exposure contributes to multiple changes in phenotype and proteome that are frequently observed in *P. aeruginosa* CF lung chronic infection isolates. This suggests that hypoxia is driving these adaptations, at least in part, and opens a new path to treatment.

Author Summary

Opportunistic antibiotic-resistant bacterial infections are an increasing threat, particularly for immunocompromised individuals such as people with cystic fibrosis (CF). These infections increase disease severity, the number of deaths and healthcare costs. *Pseudomonas aeruginosa* is a major pathogen in this context, causing persistent infections, yet the mechanisms driving its adaptation towards chronic colonisation in the CF lung are not understood.

We investigated the adaptations that *P. aeruginosa* exposed to low oxygen conditions (an important environmental pressure in the CF lung) for 28 days, to examine whether it drives adaptations that lead to chronic infection. We found that prolonged exposure to hypoxia induced stable changes in *P. aeruginosa*, which are distinct from those reported after short term exposure. We observed multiple adaptations in hypoxia adapted cultures, many of which were associated with important signalling networks linked to lifestyle shifts in bacteria and several were also observed in isolates that had adapted to chronic infection. Similar adaptive responses in other opportunistic environmental pathogens suggest that this process of adaptation could be targeted to create universal therapeutic approaches preventing antibiotic overuse and improving patient outcomes.

59 # Introduction

60 Antibiotic-resistant bacterial infections are a growing threat to society. They were associated with
61 nearly five million deaths in 2019 (1), and are expected to cause more than 10 million deaths
62 annually by 2050 (2). Opportunistic pathogens such as *Pseudomonas aeruginosa* play a crucial role
63 in escalating this crisis. While these bacteria typically do not cause infections in healthy people,
64 immunocompromised individuals and people with underlying conditions such as cystic fibrosis (CF)
65 and chronic obstructive pulmonary disease (COPD) or those on ventilator support are at great risk of
66 developing chronic *P. aeruginosa* lung infections (3,4). Moreover, opportunistic pathogens are
67 responsible for the majority of healthcare-associated infections, contributing to increasing
68 morbidity, mortality and costs (5).

69 *P. aeruginosa* is a Gram-negative opportunistic human pathogen, which is a leading cause of
70 nosocomial infections, constituting 11-26% of ventilator-associated pneumonia globally (6). Overall,
71 it causes more than 7% of all health-associated infections and is a major contributor to morbidity
72 and mortality among people with CF (7–9). It has many intrinsic and acquired mechanisms of
73 antibiotic resistance contributing to its spread and persistence (10), and the prolonged antibiotic
74 treatments necessary to manage *P. aeruginosa* chronic infections contribute to the spread of
75 antimicrobial resistance (11,12). Furthermore, the World Health Organisation recognised *P.*
76 *aeruginosa* as a high priority pathogen in 2024 while the European Centre for Disease Prevention
77 and Control (ECDC) considers it a serious threat (13–16).

78 A key feature of *P. aeruginosa* is its exquisite metabolic flexibility and adaptability to harsh
79 conditions, allowing it to transition from the colonisation of the rhizosphere or hydrosphere to
80 colonising niches within human or animal hosts, and establishing persistent infections (4,17). *P.*
81 *aeruginosa* chronic infection isolates show multiple changes that attenuate virulence, allowing it to

82 avoid immune recognition, thereby enhancing survival, and consequently, chronic infections are
83 extremely difficult to eradicate (18). Its adaptability is driven by a complex regulatory network
84 involving transcriptional regulators, DNA modifications, non-coding RNAs, quorum sensing, and a
85 range of virulence factors (18–23). These adaptations and associated lifestyle changes are also
86 driven by the alterations in c-di-GMP second messenger levels (24–27). Despite this extensive
87 research, the mechanism(s) enabling *P. aeruginosa* to transition from acute to chronic infection
88 remain unclear.

89 *P. aeruginosa*, a facultative anaerobe, thrives under low oxygen and anaerobic conditions
90 using alternative terminal electron acceptors and fermentation substrates. It preferentially colonizes
91 hypoxic niches within mucus layers of the lung over more oxygenated surfaces (28). *P. aeruginosa*
92 responds to changes in oxygen availability via the transcriptional regulator Anr, which regulates
93 many genes shown to be altered in CF chronic infection (29,30). Studies on another CF-associated
94 pathogen, *Burkholderia cenocepacia* have shown that 40% of proteins encoded within a low oxygen
95 activated (Lxa) locus showed increased abundance in chronic infection isolates from CF patients
96 (31). Subsequent studies showed that deletion of single genes from the Lxa or the entire locus
97 resulted in changes in phenotypes crucial for the virulence of this bacterium including host cell
98 attachment, intracellular survival and stress responses (31–33). Additionally, the *sicX* sRNA has been
99 proposed to be a biomarker of *P. aeruginosa* chronic infection and is also oxygen responsive (34).
100 Given that hypoxia is an important environmental pressure in the CF lung, we wanted to evaluate
101 the impact of long-term hypoxia exposure on *P. aeruginosa.*

102 We developed an experimental evolution approach and demonstrate that the impact of
103 long-term exposure to low oxygen on the proteome and phenotype of *P. aeruginosa* is consistent
104 with many adaptations that are associated with chronic lung infection. We specifically evaluated on
105 the proteome and phenotype to focus on the effective changes in the strains following long-term

106 hypoxia, which is not widely studied. Our findings provide new insights into the mechanisms that
107 underlie the persistence and pathogenesis of *P. aeruginosa* in chronic infection and possibly other
108 opportunistic pathogens, within the host.

109 Results

110 Design and Optimisation of Experimental Adaptation

111 To investigate the impact of long-term exposure to low oxygen conditions on the adaptation of *P.*
112 *aeruginosa*, we designed an experimental evolution/adaptation approach (Fig 1A), exposing the *P.*
113 *aeruginosa* early infection strain AMT 0023-30 to either 6% oxygen or to normoxia (21%) for 28
114 days. AMT 0023-30 is a well-characterised and sequenced CF paediatric early infection strain that
115 was selected from the international *P. aeruginosa* panel (35–38). This strain was isolated from a 6
116 month old paediatric patient with no former history of *P. aeruginosa* infection, thus the likelihood of
117 preadaptation to the lung or hypoxic niches is very low. Furthermore, a sequential, 96-month,
118 chronic infection strain is available (AMT 0023-34) which has also been sequenced and well
119 characterised (35–38). This strain is the ancestor of the adapted cultures further described in this
120 manuscript (Table 1). After considering the ranges of oxygen that *P. aeruginosa* is exposed to in soil
121 and water, together with the range of hypoxic conditions reported in the CF lung and available
122 literature on physiological tissue hypoxia (28,39,40), we chose 6% oxygen as a low oxygen
123 concentration. Soil aeration ranges from 10 to 20% but decreases with depth and microoxic and
124 anoxic niches are available (39). Similarly a range of oxic, hypoxic and anoxic conditions have been
125 reported for CF patient lungs (28, 40) ranging from180 mmHg in the lumen to 2.5 mmHg within the
126 mucus. Thus 6% O_2 is in the higher hypoxia range and it allowed us to observe the response to
127 hypoxia, while not excessively stressing the cells, so that we can distinguish this response from
128 changes associated with anoxia.

129 **Figure 1. Long-term adaptation of *Pseudomonas aeruginosa* to hypoxic conditions.** Experimental evolution
130 study design (**A.**) and influence of hypoxia on small colony variants emergence (**B.-D.**). **A.** Experimental
131 evolution study design. The overnight culture of the ancestral strain was inoculated into three flasks with
132 hypoxia or normoxia equilibrated medium and incubated with agitation in 6% O_2 or 21% O_2. Every 24 h 5% of
133 the culture was transferred into a fresh portion of equilibrated media. The transfers of the hypoxia-adapting
134 cultures were performed under hypoxic conditions to avoid oxygen level fluctuation. The samples from the
135 cultures adapted for 28 days were taken for further proteomic and phenotypic analysis. The details of the
136 procedure are described in the method section. **B.** Hypoxia-adapted colony morphotypes observed
137 throughout the long-term adaptation. **C.** Percentage of SCVs in individual normoxia- and hypoxia adapting
138 cultures over 28 days. **D.** Ratios of SCV 1 and SCV 2 in the hypoxia-adapting populations over 28 days. The
139 percentage of the small colony variants in the whole populations was carried out for each flask individually
140 each day.

141 To maintain stable growth over the period of the evolution experiment, daily culture transfer
142 volumes were optimised by evaluating a range of volumes (1-10%) of overnight *P. aeruginosa*
143 cultures transferred into fresh media and analysing their growth patterns (S1 Figure). A 5% volume
144 transfer was chosen as optimal, as it allowed the transfer of the maximum number of bacterial cells
145 without disrupting the growth pattern and resulted in a starting OD_{600} of ~0.1. Examination of
146 growth patterns of the early infection strain revealed small differences in the generation times
147 observed during hypoxic and normoxic conditions, with the strain growing 1.8-fold slower under
148 hypoxia (g = 107 minutes) compared to normoxia (g = 60 minutes), and showing logarithmic phases
149 of 3 h in normoxia and 6 h in hypoxia (S2 Figure). Consequently, we estimate that during the 28 day
150 adaptation period, all the cultures underwent 84-94 generations.

151 To facilitate further investigation, including phenotyping and proteome analysis, three
152 independent flasks were inoculated and incubated under either 6% oxygen or normoxia (21% O_2),
153 and samples were collected every day over 28 days, at the time of culture transfer. Three replicate
154 cultures were chosen for each condition to facilitate deeper analysis over a broad range of
155 phenotypes. To maintain stable hypoxic conditions and avoid exposure to fluctuating oxygen levels,
156 the transfers of hypoxia-adapting cultures were conducted within the hypoxic chamber. The three

157 28 day independently adapted populations evolved from the ancestral AMT 0023-30 strain are
158 referred to as N1, N2, and N3 for replicate normoxia-adapted control populations (NACs) and H1,
159 H2, and H3 for the three replicate hypoxia-adapted cultures (HACs) (Table 1). All characterisation of
160 the individual adapted populations (both HACs and NACs) was performed under normoxic
161 conditions, to ensure the observed changes were stable in the absence of continued hypoxia and
162 are not a transient, plastic response.

	Strain/Population Name	Description	Source
	E	Paediatric (6-month old) early infection cystic fibrosis strain AMT 0023-30. Ancestral strain.	(38)
	L	Paediatric late infection cystic fibrosis strain AMT 0023-34, sequential (96 months) isolate of AMT 0023-30.	(38)
NACs	**N1**	28 day normoxia-adapted population, replicate 1. Evolved from AMT 0023-30 (E).	This study
	N2	28 day normoxia-adapted population, replicate 2. Evolved from AMT 0023-30 (E).	This study
	N3	28 day normoxia-adapted population, replicate 3. Evolved from AMT 0023-30 (E).	This study
HACs	**H1**	28 day hypoxia-adapted population, replicate 1. Evolved from AMT 0023-30 (E).	This study
	H2	28 day hypoxia-adapted population, replicate 2. Evolved from AMT 0023-30 (E).	This study
	H3	28 day hypoxia-adapted population, replicate 3. Evolved from AMT 0023-30 (E).	This study

163 **Table 1. List of strains and populations used in this study**

164 Changes in colony morphology and pyocyanin production during
165 adaptation

166 Changes in colony morphology often serve as key indicators of adaptation to the environment.
167 Plating of daily samples from the adapting cultures showed the emergence of small colony variants
168 (SCVs) in both NACs and HACs; however, the SCVs appeared earlier in HACs over the timeframe (Fig
169 1B and 1C). SCVs first appeared on day 2 in the H3 population, and by day 3 in the H1 and H2
170 populations. The SCV abundance peaked at 98% on day 22, with 77% remaining on day 28 in H1. A
171 similar profile was shown in H2, with SCVs comprising 82% of the population by day 20. In contrast
172 in population H3, the SCV abundance was generally lower and more variable, reaching only 50% of
173 the population by day 15, and falling to 1% on day 21 (Fig 1C). The SCVs appeared much later in

174 normoxic cultures, on days 6, 7 and 8 in flasks N1, N2 and N3 respectively, and only reached a
175 maximum of 25-33% of the population by day 14 (Fig 1C).

176 Two distinct SCV morphologies were observed (Fig 1B and 1D). The first type, termed SCV 1,
177 was observed both under normoxia and hypoxia, and resembled the morphology most often
178 described as a rugose small colony variant characterised by small size, irregular edges and a heavily
179 wrinkled, dry surface (41). The second type, SCV 2, was bigger than SCV 1 with a similar rough, dry
180 surface; however it was easily distinguished by a more regular edge and shape and importantly, it
181 was exclusive to HACs. The SCVs were stable after replating in normoxic conditions, although SCV 2
182 morphology differed, with a smoother surface and edges (S3 Figure).

183 Throughout the 28 days of adaptation, we also observed dynamic changes in culture colour
184 (Fig 2A), suggesting changes in pigments, such as pyocyanin. Despite almost no visible change in
185 colour being observed on day 28 (Fig 2A), quantification of pyocyanin production revealed that
186 populations H1, H2 and one NAC (N1) produced comparable pyocyanin levels at day 28 to the late
187 infection strain (AMT 0023-34) (Fig 2B and Fig 2C). Although pyocyanin was higher in the NACs
188 overall compared with HACs, the differences between biological replicates suggests that pyocyanin
189 production is independent of environmental oxygen levels or is not stable in normoxic conditions.

190 **Figure 2. Influence of hypoxia on pyocyanin production. A.** Representative photographs of flasks during the
191 28 day experimental evolution study showing changes in pyocyanin production. **B. and C.** Quantification of
192 pyocyanin production by individual populations **(B.)** and mean values for normoxia- and hypoxia-adapted
193 cultures **(C.)** at 28 days, relative to early (E) and late (L) infection strains**.** The data represent the
194 concentration of pyocyanin in 1ml of bacterial culture, calculated as described in the methods. The data
195 represent two independent experiments performed in normoxic conditions, with at least three technical
196 replicates for each strain. Statistically significant differences were determined by ordinary one-way ANOVA
197 test compared to the early infection strain with an uncorrected Fishers LSD test (B.) or Kruskal-Wallis
198 one-way ANOVA test comparing all groups with an uncorrected Dunn's test (**C.**) are shown (**p< 0.01;
199 ***p<0.001; ****p< 0.0001). E: early infection clinical strain; L: late infection clinical strain; N1, N2, N3: 28-
200 day normoxia-adapted populations; H1, H2, H3: 28-day hypoxia adapted populations.

201 ## Influence of hypoxia on the whole proteome

202 The proteomes of 28 day adapted cultures were analysed to elucidate the overall influence
203 of long-term hypoxia on *P. aeruginosa*. The individual flasks were treated as biological replicates,
204 thus showing the global changes across three independent populations. Principal component
205 analysis (PCA) showed a clear adaptation to the conditions tested, PC1 and PC2 accounted for 84.0%
206 and 7.3% of the total variance respectively (Fig 3A). A total of 257 proteins showed significant
207 differences (adjusted p-value ≤0.10) in abundance between HACs and the ancestor strain, NACs and
208 the ancestor strain and/or between HACs and NACs (Table 2, S4 Table). The majority of proteins that
209 were altered in abundance between HACs, and the ancestral strain were decreased following
210 exposure to hypoxia (n=106; 72.55%), while only 36 proteins (27.45%) showed increased abundance
211 (Table 2, volcano plot, Fig 3C). An additional 13 proteins were identified as significantly altered in
212 abundance after comparing HACs to NACs. Eighty proteins were changed both in HACs and NACs
213 relative to the ancestral strain and, suggesting they may be affected by long-term culture generally
214 and not hypoxia. A total of 89 proteins were further considered as significantly altered during
215 hypoxia adaptation (Fig 3B).

216 **Table 2. Proteome comparison of 28 day the *P. aeruginosa* HACs and NACs vs the early infection**
217 **ancestral strain and HACs vs NACs.**

Protein groups	Number of proteins*
Total number of identified proteins across the ancestral strain, HACs and NACs	1788
Proteins with significantly changed abundance one-way ANOVA (p-value ≤0.05))	749
Proteins with significantly changed abundance in at least one of the comparisons with an adjusted p-value ≤0.1	257
Proteins significantly changed in abundance in HACs vs ancestral strain	142
Proteins significantly changed in abundance in NACs vs ancestral strain	169
Proteins significantly changed in abundance in HACs vs NACs	25
Proteins absent across all replicates in at least one group	117
Proteins with a significantly increased abundance in HACs vs the ancestral strain	36
Proteins with a significantly decreased abundance in HACs vs the ancestral strain	106

218 *The proteins with significantly changed abundance were determined using mean LFQ intensities of three independent populations
219 of the ancestral, early infection strain, NACs and HACs. One-way ANOVA (p≤0.05) was combined with a FDR adjustment using the
220 Benjamini-Hochberg method. An adjusted p-value cutoff of 0.1 was used.

221 **Figure 3. Whole proteome comparison of long-term hypoxia-adapted and normoxia-adapted *P.***
222 ***aeruginosa.*** **A.** Principal component analysis plot of quantified proteins from label-free LC-MS/MS analysis of
223 whole cell extracts from *P. aeruginosa* adapted to hypoxic conditions (HACs) or normoxic conditions (NACs)
224 for 28 days and the ancestral strain (D0). The PCA plot was performed using LFQ intensities of 1785 proteins
225 across three biological replicates per condition. Clustering by condition indicates specific global proteomic
226 shifts associated with long-term hypoxia adaptation. The PCA plot was generated using the Galaxy server v
227 3.4.0 (42) with ggplot2 using default settings with Euclidean distance clustering. **B.** A Venn diagram of the
228 number of proteins significantly changed in abundance between HACs and the ancestral strain; NACs and
229 the ancestral strain; and HACs vs NACs. The analysis was performed using one-way ANOVA with Benjamini-
230 Hochberg correction and proteins with an adjusted p-value <0.1 were considered significantly altered in
231 abundance. The 89 proteins in the coloured sections were considered for further analysis. The white sections
232 were not considered due to lack of relevance to hypoxia adaptation. Only the numbers in parenthesis in the
233 cross section of NACs and HACs compared to the ancestral strains were considered due to distinct change
234 between HACs and NACs (1.5 fold-change). **C.** Volcano plot of differentially expressed proteins between
235 HACs vs the ancestral strain (D0) representing $\log_{10}$ of adjusted p-values and $\log_2$ transformed fold-change
236 values. Proteins significantly decreased in abundance are highlighted in red and proteins significantly
237 increased in abundance are highlighted blue. Examples of proteins of interest are labelled. A value of 1 was
238 imputed for all the zero LFQ values, thus they are represented on the plot, despite the lack of detection. **D.**
239 STRING-based KEGG pathway enrichment of 89 proteins significantly altered in abundance in HACs vs the
240 ancestral strain and HACs vs NACs. Enrichment analysis was conducted using STRING functional enrichment
241 (FDR <0.05) (v12.0) (43). The dot plot shows the top 10 enriched pathways, where dot size corresponds to
242 the number of hits per pathway and colour represents statistical significance (FDR-corrected p-value). The
243 pathways are grouped by similarity (0.8). **E.** and **F.** Dot plots representing functional GoTerm Biological
244 Process enrichment of proteins with increased (E) and decreased abundance (F). Size corresponds to the
245 number of hits per pathway and colour represents statistical significance. The enrichment analysis and dot
246 plot were prepared using ShinyGo v0.82 (44).

247 Proteins unique to hypoxia or normoxia

248 Interestingly, 117 (15.62%) of the 749 proteins that showed significant changes in abundance (one-
249 way ANOVA) were undetectable in at least one of the groups: all three HACs, all three NACs or all
250 three ancestral strain replicates. Their consistent presence or absence suggests that their expression
251 was either switched on or off, and consequently, they are likely to play critical roles under the
252 specific conditions. Among these, only three proteins were unique to HACs and not detected in any

253 NAC or in the ancestral strain: phenazine biosynthesis protein, PhzE; Pel polysaccharide secretion
254 protein, PelC; and glutamine amidotransferase, HisH2 (Table 3). Additionally, anthranilate synthase
255 component I PhnA and iron(II)/α-ketoglutarate-dependent oxygenase AmbC, involved in toxin
256 production were undetected in the ancestral strain, and expressed in all three HACs, but only one of
257 the NACs.

258 Many proteins that were undetectable in HACs but expressed in the ancestral strain and all
259 NACs and thus potentially redundant in low oxygen conditions, are involved in virulence, including
260 flagellar hook protein FlgE, involved in motility, virulence, host interactions, biofilm formation and
261 antibiotic resistance; lipid A-disaccharide synthase LpxB, involved in immune evasion; spermidine
262 dehydrogenase SpdH, involved in chemotaxis and motility. In addition, GacS and ColR, components
263 of two-component response regulator systems involved in virulence regulation, and phospholipase
264 B were also undetectable in all HACs, but were present in two of the replicates of the ancestral
265 strain, and all three NACs. Moreover, oxidoreductase MexS associated with antibiotic resistance and
266 virulence factor production, chromosome partitioning protein MksE, and iron-sulphur cluster
267 assembly protein CyaY were detected in all replicates of the ancestral strain and two of the NACs,
268 while undetectable in all three HACs (Table 3). This attenuation of virulence proteins mirrors the loss
269 of virulence during chronic infection.

270 Proteins which were detected both in the ancestral strain and HACs but not detected in
271 NACs may also be important in the process of adaptation to hypoxia, as their abundance is
272 maintained. The transcription termination factor Rho associated with biofilm formation and stress
273 resistance, and UDP-N-acetylglucosamine acyltransferase LpxA belong to this group. Additionally,
274 polymer-forming cytoskeletal protein PA0664 involved in biofilm formation, and L-lactate
275 dehydrogenase LldD were detected in all replicates of the ancestral strain and two of the HACs, but
276 none of the NACs, suggesting their maintenance is required for fitness under low oxygen. Lastly, the

277 proteins which were undetected in the ancestral strain replicates and all HACs include the acyl-
278 homoserine lactone synthase LasI which produces a quorum-sensing signal and positively regulates
279 numerous *P. aeruginosa* virulence-associated traits including biofilm formation, oxidative stress
280 resistance and elastase production. Additionally, lipase PA1615 and transcriptional regulator PchR,
281 controlling pyochelin production were not detected in all replicates of the ancestral strain and in
282 two of the HACs while expressed in all three NACs. Interestingly, the Anr transcriptional regulator
283 was undetectable both in normoxic and hypoxic conditions.

284 **Table 3. Examples of proteins not detected in at least one of the groups (Day 0, HACs, NACs).**

Gene ID[a]	Protein Name	Protein Product Name	D0[b]	HACs[b]	NACs[b]	Function	NP[c]	MW[d]	SC[e]
PA3062	**PelC**	**PelC**				Exopolysaccharide (EPS) production, Biofilm formation (45)	6	18.7	58.1
PA1903	**PhzE2**	**Phenazine biosynthesis protein**				Pyocyanin production (46)	4	69.0	7.3
PA3152	**HisH2**	**Glutamine amidotransferase**				Amino acid biosynthesis (47)	5	22.7	38.6
PA1001	PhnA	Anthranilate synthase component I				QS, pyocyanin production (48)	6	58.7	14
PA2304	AmbC	Iron(II)/α-ketoglutarate-dependent oxygenase				Toxin production, virulence (49)	7	40.7	27.9
PA5139	**PA5139**	**Hypothetical protein**				Biofilm formation, Stress resistance (50)	7	27.6	32.3
PA3644	**LpxA**	**UDP-N-acetylglucosamine acyltransferase**				LPS production (51)	8	28.0	34.9
PA0664	PA0664	Polymer-forming cytoskeletal protein				Biofilm formation (52)	2	14.8	23.6
PA4771	LldD	L-lactate dehydrogenase				Stress resistance, persistence (53)	16	41.1	45.7
PA1080	**FlgE**	**Flagellar hook protein FlgE**				Host interaction, virulence, biofilm formation, antibiotic resistance, motility (54–56)	2	48.3	7.4
PA1157	**PA1157**	**Probable two-component response regulator**				Two component system, regulator (57)	3	26.4	13.1
PA3643	**LpxB**	**Lipid A-disaccharide synthase**				LPS production, immune evasion (51)	6	41.3	23
PA3713	**SpdH**	**Spermidine dehydrogenase**				Motility, chemotaxis (56,58)	9	68.9	19.5
PA4381	ColR	Two-component response regulator ColR				Virulence (57,59,60)	2	25.2	16.3
PA0928	GacS	Sensor/response regulator hybrid				QS, virulence, SCVs (61,62)	5	101.1	8.2
PA2927	PlaB	Phospholipase B				Biofilm formation (63)	4	49.5	5.2
PA2491	MexS	Oxidoreductase MexS				Antibiotic resistance, virulence, pyocyanin production, rhamnolipid production (64–67)	10	36.8	44.2
PA5275	CyaY	Iron-sulphur cluster assembly protein				Iron homeostasis (68)	4	11.9	41.7
PA1432	**LasI**	**Autoinducer synthesis protein LasI**				QS, Elastase production, virulence (69,69,70)	3	22.7	20.4
PA1615	PA1615	Probable lipase				Lipase activity (69)	1	12.5	21.2
PA4227	PchR	Transcriptional regulator PchR				Pyochelin production (70)	3	32.3	14.9
PA1544	**Anr**	**Transcriptional regulator Anr**				Anaerobic metabolism regulation (71)	4	27.1	15.6

285 [a]Gene ID – *P. aeruginosa* PAO1 gene locus ID
286 [b]H/N – Dark blue: protein detected in all three replicates; light blue: protein detected in two out of three replicates; light orange:
287 proteins not detected in two out of three replicates; Dark orange: Protein not detected in all three replicates.
288 [c]NP - Unique peptides: The number of peptide sequences unique to a protein
289 [d]MW - Molecular weight as determined by Q-Exactive LC-MS using *P. aeruginosa* PAO1 reference
290 [e]SC - % sequence covered by matching peptides for the identified protein
291 Proteins consistently absent or consistently present in all three replicates the ancestral strain HACs and NACs are marked in bold

292 **Functional enrichment**

293 Functional enrichment analysis of the 89 proteins identified in the previous step (Fig 3B) was
294 performed. GO biological process identified 53 enriched categories (S5 Table), including various
295 processes associated with carbon, nitrogen and amino acid metabolism; fatty acid and lipid
296 metabolism; nucleotide and ribonucleotide metabolism. A separate analysis of proteins with
297 increased or decreased abundance in HACs provided further insights into these processes (S5
298 Table). Overall, 25 GO biological processes were enriched among proteins increased abundance in
299 hypoxia (Fig 3E), while 27 processes were enriched in the decreased abundance group (Fig 3F).
300 Hypoxia led to upregulation of processes related to ribonucleotide metabolism, but a
301 downregulation of pyrimidine-containing compound metabolism. Additionally, processes associated
302 with lipid and fatty acid metabolism, oxidation-reduction and chromosome segregation were
303 upregulated in HACs. Multiple processes associated with amino acid metabolism were also
304 downregulated including glutamine and arginine. Additionally, nitrogen metabolism associated
305 processes were downregulated as well. KEGG pathway enrichment analysis further highlighted
306 alterations of pyrimidine metabolism, changes of RNA degradation pathways, and various carbon,
307 amino acid, and energy metabolism associated pathways (Fig 3D).

308 Antibiotic resistance of adapted cultures

309 A change in the abundance of many proteins associated with the resistance to multiple classes of
310 antibiotics was observed in HACs (Table 4). Six proteins were increased in abundance including UDP-
311 N-acetylmuramate-alanine ligase MurC, outer membrane protein H1 precursor OprH, and the
312 Topoisomerase IV subunit A ParC, while five were decreased in abundance.

313 **Table 4. Examples of proteins altered in abundance in *P. aeruginosa* in three comparisons.**

			Fold-change[b]						
Gene ID[a]	Protein Name	Protein Product Name	HACs vs D0	NACs vs D0	HACs vs NACs	Function[c]	NP[d]	MW[e]	SC[f]

PA1903	phzE2	phenazine biosynthesis protein PhzE	30383.00	---	30383.00	Pyocyanin and phenazine biosynthesis (46,72)	4	69.0	7.3
PA2444	glyA2 / ShrA	serine hydroxymethyltransferase	21.96	---	---	SCVs, biofilm formation, EPS production, motility, redox control (73)	10	45.0	47.6
PA3559	PmrE	probable UDP-glucose dehydrogenase	21.53	---	---	EPS production, antibiotic resistance, LPS modification (74,75)	3	51.8	10.6
PA1327	PA1327	probable protease	11.20	---	---	Protease activity	12	72.5	20.3
PA3723	PA3723	probable FMN oxidoreductase	5.46	---	---	Stress resistance, antibiotic resistance (76)	24	40.3	80.4
PA4547	PilR	two-component response regulator PilR	4.52	---	---	Motility, virulence (58)	4	49.7	13.3
PA4411	MurC	UDP-N-acetylmuramate--alanine ligase	3.05	---	---	Antibiotic resistance, peptidoglycan biosynthesis (77,78)	13	52.0	25.8
PA1772	RraA	probable methyltransferase. Ribonuclease activity regulator protein	2.64	---	---	RNA turnover, global regulator (79)	11	17.4	67.3
PA0083	TssB1	TssB1	2.46	---	---	Antibiotic resistance, T6SS (80)	13	18.8	73.8
PA1178	OprH	PhoP/Q and low Mg^{2+} inducible outer membrane protein H1 precursor	2.17	---	---	Antibiotic resistance (81)	23	21.6	69
PA4964	ParC	Topoisomerase IV subunit A	1.77	---	---	Antibiotic resistance (82,83)	18	83.4	34.4
PA0141	Ppk2	conserved hypothetical protein	---	---	1.88	Antibiotic resistance (84)	20	40.8	72.8
PA3262	PA3262	probable peptidyl-prolyl cis-trans isomerase, FkbP-type	---	---	1.74	Virulence; peptidoglycan biosynthesis (85)	21	26.8	48.6
PA4542	ClpB	ClpB protein	---	---	1.37	Stress resistance, virulence (86)	72	95.0	70.3
PA4163	Tse8	hypothetical protein	-2.29	---	---	Virulence (87)	20	60.5	49.6
PA0428	RhlE2	probable ATP-dependent RNA helicase	-2.38	---	---	RNA turnover, global regulator, virulence (72)	30	70.1	51
PA2991	Sth	soluble pyridine nucleotide transhydrogenase	-2.61	---	---	Redox control (88)	30	51.2	64.9
PA2667	MvaT/ MvaU	MvaU	-2.68	---	---	Virulence, pyocyanin prod., motility, protease prod., biofilm formation, QS (89–91)	19	13.4	87.2
PA3083	PepN	aminopeptidase N	-4.26	-2.38	---	Virulence, competition (92)	45	100.1	41.5
PA5078	OpgG	OpgG	-4.44	-2.79	---	Stress resistance, biofilm formation (93)	14	59.5	34.9
PA3831	PepA	leucine aminopeptidase	-5.07	---	---	Virulence, protein turnover (94)	33	52.3	71.1
PA5507	PA5508	hypothetical protein	-5.56	---	---	QS (95)	12	24.3	68.2
PA0301	SpuE	polyamine transport protein	-6.02	---	---	TSS3 regulation, virulence (96,97)	12	40.1	55.9
PA0423	PasP	lipocalin protein family member	-6.04	---	---	Antibiotic resistance, virulence (98,99)	17	20.8	73.3
PA1847	NfuA	NfuA	-7.77	---	---	Stress resistance, iron homeostasis, virulence (100,101)	8	21.1	47.9
PA3470	PA3470	NUDIX hydrolase	-105969.67	---	---	Antibiotic & stress resistance, pyocyanin prod (102)	3	16.7	13.2
PA3115	FimV	motility protein FimV	---	---	-1.40	Motility, T2SS (103,104)	23	96.9	27.4
PA4427	SspB	stringent starvation protein B	---	---	-5.65	Antibiotic resistance, virulence Iron homeostasis, QS (105)	3	14.5	47.4
PA4525	PilA	type 4 fimbrial precursor PilA	---	---	-13.11	Virulence, biofilm formation, motility (58,106)	1	15.5	19.5
PA2927	PlaB	phospholipase B	---	---	-23843.67	Biofilm formation (63)	4	49.5	5.2

Blue shading represents proteins increased in abundance or unique to hypoxia. Dark blue: ≥5-fold increase in abundance; medium blue: 2- to 5-fold increase in abundance, light blue: 1.5- to 2-fold increase in abundance. Orange shading represents proteins decreased in abundance in hypoxia or absent in hypoxia. Dark orange: ≥5-fold decrease in abundance; medium orange: 2- to 5-fold decrease of abundance; light orange: 1.5- to 2-fold decrease in abundance.

[a]Gene ID – *P. aeruginosa* PAO1 gene locus ID.

[b]Proteins not significantly altered in abundance between given conditions are marked as "---"

[c]Relevant protein function assigned by literature searches, UniProt Database or Pseudomonas Genome Database.

[d]NP - Unique peptides: The number of peptide sequences unique to a protein

[e]MW - Molecular weight as determined by Q-Exactive LC-MS using *P. aeruginosa* PAO1 reference (kDa)

[f]SC - % sequence covered by matching peptides for the identified protein

324 We examined whether the alterations in protein abundance associated with antibiotic
325 resistance affect affected antibiotic susceptibility of adapted cultures. Changes in sensitivity to a
326 wide range of their antibiotic classes were observed in both HACs and NACs compared to the early
327 infection strain (Fig 4A and 4B). However, both H1 and H2 populations clearly showed greater
328 antibiotic resistance than NACs or ancestral cultures, correlating with the relative changes in protein
329 abundance. Increased resistance to fluoroquinolones, macrolides, cephalosporins, carbapenems
330 and penicillins was observed in both H1 and H2 cultures, together with decreased resistance to
331 aztreonam. Interestingly, the H3 culture only showed an increased resistance to aztreonam with no
332 change in susceptibility to any other antibiotic tested. All strains were resistant to tetracycline.

333 **Figure 4. Effects of long-term hypoxia adaptation on antibiotic resistance and stress resistance**. **A.** Graphs
334 represent the antibiotic susceptibility of early infection control strain AMT 0023-30, late infection strain,
335 AMT 0023-34, and 28-day adapted populations using diffusion discs, tested in normoxic conditions. Bars
336 represent the mean inhibition zone diameter. The data represent three biological replicates and error bars
337 represent the standard deviation. The statistical significance was determined with the nonparametric
338 Kruskal-Wallis test in combination with uncorrected Dunns multiple comparisons test (*$p< 0.05$; **$p< 0.01$;
339 ***$p<0.001$; ****$p< 0.0001$). **B**. Summary of antibiotic resistance to all tested antibiotics. **C.** Determination
340 of stress resistance with droplet assays. Representative pictures of colonies from serial dilutions of each
341 strain plated on agar with the specific stress factor added. The experiments were performed in normoxic
342 conditions at least three times for each stress type with the early infection strain as a control. **D.** Table
343 summarising changes in stress sensitivity. ↑ - increased resistance; ↓ - decreased resistance; = no significant
344 difference in resistance; R – no inhibition zone observed. E: early infection clinical strain; L: late infection
345 clinical strain; N1, N2, N3: 28-day normoxia-adapted populations; H1, H2, H3: 28-day hypoxia adapted
346 populations.

347 Hypoxia-adapted cultures show changes in stress response

348 Many proteins related to stress responses showed changes in abundance in response to long-term
349 exposure to hypoxia (Table 4), including the osmotic stress response associated protein, OpgG, and
350 the oxidative stress response associated protein, PA3723. The hypothetical protein, PA5139

351 previously associated with stress resistance, and lactate dehydrogenase LldD, associated with
352 oxidative stress resistance were detected in the ancestral strain and HACs, but not any of the NACs.

353 To examine the impact of these alterations on the phenotype of each of the individual
354 populations, droplet stress plates were prepared to test a range of stresses described as hallmarks
355 of the CF lung environment. No clear pattern of resistance to high temperature, osmotic or acidic
356 stress between the HACs and NACs was observed (Fig 4C and 4D). Interestingly, increased resistance
357 to oxidative stress was observed in both H1 and H2 cultures and in the N3 culture, which were also
358 the only populations where SCVs had been detected on day 28, and where increased biofilm
359 production and exopolysaccharide production were observed.

360 Hypoxia-adapted cultures show increased biofilm formation and 361 exopolysaccharide production

362 Typically, anaerobic conditions promote biofilm formation, with greater numbers of live bacteria,
363 increased thickness, and more compact structures (107). In this work, changes in the abundance of
364 proteins associated with biofilm and/or exopolysaccharide production were also observed in
365 response to exposure to 6% oxygen (Table 3 and Table 4). Two proteins associated with biofilm
366 associated antibiotic resistance were increased in abundance, while three were decreased.
367 Additionally, some of the proteins associated with biofilm formation or EPS production were not
368 detected in at least one of the groups: exopolysaccharide export protein, PelC, was identified solely
369 in HACs but not in NACs or ancestral strain (Table 3); solute-binding protein, PA5139, is present in
370 the ancestral strain, maintained in HACs, while undetectable in NACs; the polymer-forming
371 cytoskeletal protein PA0664 is detected in the ancestral strain, and in two HACs, but none of the
372 NACs; phospholipase PlaB was detected in two replicates of the ancestral strain, detected in all of
373 the NACs, but none of the HACs.

374 To confirm the impact of these proteome changes on biofilm and exopolysaccharide
375 production, these phenotypes were examined in each individual adapted culture (Fig 5A and 5B).
376 Both H1 and H3 populations showed a significant, dramatic increase in biofilm formation as
377 compared to the early infection strain after 24 h (6.1- and 4.3-fold increases respectively).
378 Significant increases in biofilm production were also observed in the late infection strain (1.6-fold),
379 H1 (3.9-fold) and H2 (1.4-fold) over the ancestral strain at 48 h, and this trend persisted at 72h (Fig
380 5A). The increased biofilm production of the H3 population was transient and reverted to AMT
381 0023-30 early infection strain levels by 48 h. Congo Red staining revealed darker colonies for H1 and
382 H2 populations which were more wrinkly than in the other strains indicating a higher production of
383 exopolysaccharides (Fig 5B). Interestingly, a similar phenotype was observed in culture N3, again
384 suggesting that this phenotype is not solely dependent on oxygen availability.

385 **Figure 5. Effects of long-term hypoxia adaptation on biofilm formation, exopolysaccharide production and**
386 **siderophore production. A.** Biofilm formation capability of hypoxia-adapted cultures determined with the
387 crystal violet assay after 24, 48 or 72h of static incubation on a 96-well plate in normoxic conditions. Data
388 represent the mean value of the OD_{590}/OD_{600} ratio from three separate experiments with at least six
389 technical replicates for each strain. Statistically significant difference by Kruskal-Wallis one-way ANOVA test
390 compared to the ancestral, early infection strain (E) with an uncorrected Dunn's test (**p< 0.01; ***p<0.001;
391 ****p< 0.0001). **B.** Exopolysaccharide production by the adapted cultures. The photographs show colonies
392 of different populations of bacteria. The change of colour to a darker shade and a wrinkly colony surface
393 indicate a higher exopolysaccharide production. **C.** Siderophore production represented as the mean of
394 siderophore units produced by each colony forming unit, tested in normoxic conditions. Statistically
395 significant differences by ordinary one-way ANOVA test compared to the ancestral, early infection strain
396 with an uncorrected Fishers LSD test are shown (*p<0.05; **p< 0.01). E: early infection clinical strain (AMT
397 0023-30); L: late infection clinical strain (AMT 0023-34); N1, N2, N3: 28-day normoxia-adapted populations;
398 H1, H2, H3: 28-day hypoxia adapted populations.

399 Adaptation to hypoxia affected iron acquisition and homeostasis

400 Proteomic analysis showed changes in the abundance of proteins related to iron homeostasis and
401 acquisition pathways (Table 4). CyaY protein involved in iron-sulphur cluster assembly was
402 undetected in HACs but was present in the ancestral strain and maintained in the NACs (Table 3).
403 NfuA, previously associated with iron homeostasis was decreased in abundance by nearly 8-fold
404 relative to the ancestral strain (Table 4). In contrast, the stringent starvation protein SspB was
405 increased in abundance over 5-fold in HACs compared to NACs.

406 Differences in iron acquisition and siderophore levels of all individual populations showed a
407 consistent, clear decrease in siderophore production in all HACs by 2.8- to 3.6-fold but no significant
408 change in NACs (Fig 5D). No significant differences were detected in the pyochelin and pyoverdine
409 production pathways, but the PchR transcriptional regulator was undetectable in all the replicates of
410 the ancestral strain, two HACs and present in all NACs. Moreover, a 4-fold decrease in siderophores
411 was also observed between the early infection strain (ancestral) and late infection strain.

412 Adaptation to hypoxia induces changes in motility

413 A common adaptation associated with P. aeruginosa chronic infection isolates is loss of motility.
414 Multiple proteins associated with motility showed changes in abundance in the HACs. Flagellar hook
415 protein FlgE, and spermidine dehydrogenase SpdH were undetectable in the HACs while present in
416 the ancestral strains and NACs (Table 3). The two-component response regulator, PilR, and serine
417 hydroxymethyltransferase ShrA were increased in abundance in HACs (4.5 and 22.0-fold
418 respectively), but not in NACs compared to the ancestral strain. In contrast, DNA-binding protein
419 MvaT was decreased in abundance by 2.7-fold. Additionally, type 4 fimbrial precursor PilA, and FimV
420 were both decreased in abundance (13- and 1.4 fold respectively) in HACs vs NACs. Notably, many
421 of these proteins are also associated with biofilm formation and/or antibiotic resistance (ShrA,
422 MvaT, PilA, FlgE).

423 To elucidate the effect of hypoxia on motility further, the motility of the individual cultures
424 was assessed. The late infection strain showed a 2-fold reduction in swarming (Fig 6B) and a
425 moderate reduction in twitching motility (1.3-fold) (Fig 6C), while H1 and H2 showed an increased
426 swimming (1.5 and 1.2-fold) compared to the early strain (Fig 6A). All forms of motility were
427 decreased in H3 by over 2.4-fold (Fig 6A, 6B, 6C). A similar pattern was observed in culture N3, with
428 a 1.6-fold decrease in swimming motility and a 1.9-fold decrease in twitching motility (Fig 6A, 6C).
429 The pattern of swarming motility was clearly different between NACs and HACs. N1 and N2
430 populations showed classic swarming patterns with clearly distinguishable dendrites despite
431 showing no changes in diameter (Fig 6B). N3 showed a different pattern, forming colonies with
432 smooth edges. The H1 and H2 colonies on swarm plates were clearly distinguishable from the N1
433 and N2 counterparts, with no clear dendrites being formed (Fig 6). Overall, exposure to hypoxia led
434 to clear changes in strain motility.

435 **Figure 6. Effects of long-term hypoxia adaptation on *P. aeruginosa* motility and virulence in the *Galleria***
436 ***mellonella* model. A.** Changes in swimming motility**. B.** Changes in swarming motility. **C.** Changes in
437 twitching motility. For each type of motility, a graph representing the mean of diameter of the colony with
438 bars representing data from at least three separate experiments conducted in normoxic conditions, with at
439 least two technical replicates. Statistically significant difference by Kruskal-Wallis one-way ANOVA test
440 compared to the ancestral, early infection strain (E) with an uncorrected Dunn's test (*p< 0.05; **p< 0.01;
441 ***p<0.001; ****p< 0.0001). **D.** Graph representing the mean CFU required to reach a lethal dose leading to
442 50% mortality (LD50) within 24h of the experiment from at least three independent experiments**.** A touch to
443 the larvae head was used to determine if they are alive. Statistically significant difference by Kruskal-Wallis
444 one-way ANOVA test compared to the ancestral, early infection strain (E) with an uncorrected Dunn's test is
445 presented (*p< 0.05). **E.** A representative image showing the *G. mellonella* larvae melanisation. Healthy
446 larvae with no disease symptoms are a bright cream colour. Larvae showing a slightly beige colour show first
447 symptoms of infection, larvae with dark spots/stipes are clearly affected and the severely melanised larvae
448 are in the late stages of the infection or dead. E: early infection clinical strain AMT 0023-30; L: late infection
449 clinical strain AMT 0023-34; N1, N2, N3: 28-day normoxia-adapted populations; H1, H2, H3: 28 day hypoxia
450 adapted populations.

451 ## Effects of hypoxia-adaptation on *in vivo* virulence

452 Previously we showed that three different late infection CF isolates were less virulent in the *G.*
453 *mellonella* in vivo model than their earlier infection counterparts (37). HACs showed that
454 adaptation to hypoxia altered the abundance of several proteins involved in virulence, and many
455 virulence-associated phenotypes, including SCV formation, stress and antibiotic resistance, toxin
456 and LPS production, and motility. As mentioned, phenazine biosynthesis protein PhzE was unique to
457 HACs; Iron(II)/α-ketoglutarate-dependent oxygenase AmbC involved in toxin production was
458 undetectable in the ancestral strain and two of the NACs while present in all HACs. The earlier
459 mentioned two component system proteins GacS and ColR were undetectable in all HACs while
460 present in two replicates of the ancestral strain and all NACs (Table 3). Additionally, virulence
461 factors, leucine aminopeptidase PepA and lipocalin protein PasP, were decreased in abundance in
462 HACs (Table 4). Unexpectedly, no differences in virulence were observed *in vivo* in *G. mellonella*
463 between the ancestral, early infection strain and the HACs (Fig. 6D and 6E), showing hypoxia is
464 unlikely to drive this adaptation.

465 # Discussion

466 Understanding the complex network of pathway interactions and the evolutionary pressures *P.*
467 *aeruginosa* undergoes in different environments is the key to understanding its biology and the
468 mechanisms behind chronic infection, thereby, facilitating the development of effective
469 therapeutics. Hypoxic niches are abundant in the CF lung due to increased mucus thickness,
470 obstructive mucus plugging and increased oxygen consumption by epithelial and immune cells
471 (28,108,109). Studies have shown that microaerobic respiration is the predominant mode of *P.*
472 *aeruginosa* growth in the CF lung (110,111), with two transcription factors, Anr and Dnr, tightly
473 regulating the response to changes in oxygen tension (29,71,112,113).

474 While the impact of short-term severe hypoxia and anoxia on *P. aeruginosa* has been
475 previously described (114,115), the impact of moderately-low hypoxia stress has not been
476 examined over extended periods. To enable an in-depth phenotype and proteome analysis of
477 adapted cultures, we restricted the study to three replicates in each condition. This focused
478 approach allowed us to demonstrate that prolonged low oxygen conditions alone can induce stable
479 changes to the proteome and phenotype, many of which are typically associated with chronic
480 infection, and thus may facilitate the transition from acute to chronic infection.

481 Diverse patterns of adaptation to long-term hypoxia

482 We observed two distinct patterns of hypoxia adaptation in *P. aeruginosa*, with H1 and H2 adapting
483 differently from H3 (Fig. 7). This is consistent with reports on evolution of different characteristics
484 under the same environmental pressures, including bacterial populations isolated from the same
485 lung niche, or in different regions of a biofilm, and enables bacterial competitiveness (21,116–120).
486 Flynn et. al (2016), using a similar experimental evolution approach compared three biofilm cultures
487 and three planktonic cultures of *P. aeruginosa* PA14 over 90 days and determined that diverse
488 phenotypes appeared over time with different abilities to persist between replicate cultures, and
489 also between colonies isolated from the same population (117). Furthermore, the various colony
490 morphologies observed in their study correlated with temporal variations in c-di-GMP levels (117),
491 which aligns with the changes in the abundance of proteins associated with the response to c-di-
492 GMP in HACs. We will evaluate the potential genetic changes that may have led to this in a future
493 study.

494 Two of the HACs in this study (H1 and H2) showed consistent alterations across multiple
495 phenotypes, while the third population displayed only slight alterations relative to the ancestral,
496 early infection strain and was closer in phenotype to the NACs (Fig. 7). This pattern aligns with
497 earlier observations that proteome changes caused by short term hypoxia response were strain-

498 specific (115), suggesting that different adaptation patterns can occur as the population diversifies
499 over the longer term. Given the diversity of *P. aeruginosa* isolates within patients and between
500 patients, it should be noted that the late infection strain which was examined in parallel in
501 phenotyping experiments represents one branch within a potentially more complex evolutionary
502 tree in that patient. Further genetic characterisation of the populations and specific subpopulations
503 will provide additional information on diversity.

504 **Figure 7. Patterns of adaptation to long-term hypoxia.** Summary of the phenotypic changes of adapted
505 cultures tested in normoxic conditions compared to the ancestral strain AMT 0023-30 (E) and the late
506 infection strain AMT 0023-34 (L). It should be noted that L is a single clinical strain and not representative of
507 all chronic infection isolates or strains. ↑ - indicates an increase; ↓ - indicates a decrease; = indicates no
508 significant difference in resistance; L: late infection clinical isolate; N1, N2, N3: 28-day normoxia-adapted
509 populations; H1, H2, H3: 28-day hypoxia adapted populations. (121).

510 Adaptation of *P. aeruginosa* to long-term hypoxia is consistent with
511 changes observed during chronic infection

512 When oxygen availability decreases, electron transport chain efficiency also decreases, leading to
513 NADH accumulation and an increased $NADH/NAD^+$ ratio (122), creating a more reducing
514 intracellular environment (defined as redox stress) which must be mitigated to maintain cellular
515 function and viability. This is regulated by c-di-GMP signalling, which plays a central role in
516 mediating low oxygen responses and stress resistance in *P. aeruginosa* (123,124). It facilitates
517 metabolic switching in response to environmental stimuli, including the transition from a planktonic
518 to a biofilm lifestyle (24,124,125) and regulates multiple phenotypes such as EPS production,
519 motility, pyocyanin production, and antibiotic resistance (126–128).

520 Based on previous studies (113,115,129,71), we expected decreased oxygen availability
521 would lead to an increased abundance of the Anr regulator. However, in contrast, Anr was not

522 detected in any of the HACs, although it was present in the ancestral strain. Previous studies
523 investigating the Anr regulon were performed under either anoxia or severe hypoxia (0.2-2% O_2),
524 rather than the moderately-low hypoxia used here. There are three possible explanations: 1) the
525 oxygen level may be too high for Anr activity; 2) there are other levels of regulation of Anr as yet
526 undiscovered; 3) hypoxia adaptation may have selected for strains that downregulate Anr to reduce
527 energy costs. This is important in the context of the CF lungs, where oxygen gradients from anoxia
528 to physiological oxygen are present, suggesting more variable responses and adaptation
529 mechanisms than assumed in previous studies.

530 Given the absence of Anr in HACs, alternative regulatory pathways are likely, as exemplified
531 by >20-fold increase in abundance of the serine hydroxy methyltransferase, ShrA in HACs. Deletion
532 of *shrA* was previously shown to lead to increased c-di-GMP levels, emergence of SCVs, increased
533 biofilm, EPS and pyocyanin production, decreased swarming motility and suppression of iron
534 acquisition genes and denitrification operons (Fig 8A) (73) which align with many of the phenotypes
535 identified in response to long-term hypoxia. We propose that the redox imbalance caused by
536 hypoxia increases the abundance of ShrA *via* a yet unknown mechanism.

537 **Figure 8. Suggested mechanism of regulation of c-di-GMP levels by 6% oxygen hypoxia exposure. A.**
538 Mechanism of regulation of c-di-GMP levels by ShrA and the Gac/Rsm system system in normoxic conditions
539 based on available literature. When NADH/NAD+ ratio is balanced, ShrA activity leads mostly to the
540 production of (6S)-THF, which leads to limited SAM production and WspA methylation. This leads to a low
541 production of c-di-GMP by WspR. **B.** Proposed mechanism of regulation of c-di-GMP levels by ShrA and the
542 Gac/Rsm system in hypoxic conditions based on the proteomic analysis and phenotype studies presented in
543 this work. An increased NADH/NAD+ ratio may lead to a shift ShrA activity via an yet unknown mechanism,
544 which leads to an increased (6S)-5,10-CH_4-THF production, increasing SAM production and WspA
545 methylation. This leads to a increased production of c-di-GMP by WspR. Anr: anaerobic regulator; GacA:
546 response regulator; GacS: sensor kinase; LasI: acyl-homoserine lactone (AHL) synthase; LasR: Las quorum
547 sensing system transcriptional regulator; MetF: methylenetetrahydrofolate reductase; MetH: methionine
548 synthase; MetK: S-adenosylmethionine synthetase; MetY: homocysteine synthase; MvaT: hitone-like nucleoid
549 structuring global transcriptional regulator; RhlE2: Dead-boxRNA helicase; RsmA: RNA-binding regulator of

550 secondary metabolites A; RsmY: rsm system small regulatory RNA Y; RsmZ: rsm system small regulatory RNA
551 Z; SadC: suppressor of alginate production diguanylate cyclase; ShrA: serine hydroxymethyltransferase;
552 WspA: methyl-accepting chemotaxis protein; WspC: methyltransferase; WspE: histidine kinase; WspF:
553 methylesterase; WspR: diguanylate cyclase; THF: tetrahydrofolate; (6S)-THF: (6S)-tetrahydrofolate; (6S)-5,10-
554 CH_4-THF: (6S)-5,10-methylenetetrahydrofolate; SAM: S-adenosylmethionine; SAH: S-adenosylhomocysteine.
555 Green arrows indicate upregulation or activation. Red arrows indicate downregulation or inactivation. Solid
556 lines define literature described relationships. Dashed lines define hypothetical relationships. Green boxes
557 indicate proteins increased in abundance in the proteomic analysis performed as a part of this work. Red
558 boxes indicate proteins decreased in abundance in the proteomic analysis performed as a part of this work.

559 ShrA catalyses the reversible conversion of glycine and (6S)-5,10-methylene-THF ((6S)-5,10-
560 CH_4-THF) to serine and (6S)-THF, with a nearly threefold preference for the latter products (73).
561 Besides its role in c-di-GMP biosynthesis regulation, 5,10-CH_4-THF regulates folate and nucleotide
562 biosynthesis and amino acid metabolism. However, as these findings were identified under
563 normoxic conditions, ShrA's role in hypoxia remains unclear and warrants further investigation. In
564 particular, its reaction flux may be influenced by factors such as the increased NADH/NAD^+ ratio
565 observed under hypoxic conditions. Given that ShrA contributes to restoring redox balance by
566 reducing the NADH/NAD^+ ratio, its elevated abundance is likely to be beneficial under hypoxic
567 stress. The (6S)-5-CH_3-THF synthesized by ShrA is further metabolized through several steps to
568 produce S-adenosylmethionine (SAM), which serves as methyl group donor for the methylation of
569 WspA (73). Methylated WspA activates WspR and c-di-GMP synthesis (130). Thus, a shift towards
570 synthesis of (6S)-5-CH_4-THF would increase the methylation of WspA, leading to increased levels of
571 c-di-GMP under hypoxic conditions (Fig 8B). We acknowledge that ShrA regulation in hypoxia may
572 be more complex and requires further investigation, as it has been previously shown to be induced
573 by homocysteine, repressed by SAM, and activated via quorum sensing and PpyR (131,132).

574 Sensory histidine kinase GacS is also involved in c-di-GMP regulation. Under non-stress
575 conditions, GacS levels are naturally low or undetectable (61), however, when GacS is absent, less
576 GacA is phosphorylated, leading to reduced expression of RsmY and RsmZ sRNAs (133). This results

577 in a larger pool of active RsmA, increased repression of target mRNAs, and ultimately, lower c-di-
578 GMP levels. Unexpectedly, we detected GacS in the ancestral strain and NACs, but not the HACs
579 which is possibly due to the activity of regulators of RsmZ/RsmY sRNAs. Histone-like protein MvaT
580 reduces c-di-GMP levels by binding to the upstream regions of rsmY/rsmZ repressing their
581 transcription, increasing RsmA levels and repressing the activity of diguanylate cyclases (90).
582 Additionally, the RhlE2 reduces RsmY and RsmZ stability, thus promoting RsmA sequestering and
583 allowing the production of c-di-GMP (72). In HACs we observed comparable >2.5-fold decreases in
584 the abundance of MvaT, and RhlE2 compared to the ancestral strain, which was not observed in
585 NACs. Therefore, we speculate that the presence of GacS in NACs and ancestral strain is overcome
586 by the activity of RhlE2 and MvaT coupled with the decreased production of c-di-GMP by WspR.

587 Taken together, our findings suggested that the observed changes in abundance of ShrA,
588 GacS, RhlE2 and MvaT lead to an increase in cellular c-di-GMP levels, consistent with the observed
589 phenotypes including increased biofilm and EPS production, emergence of stable SCV phenotypes,
590 alterations in motility, antibiotic resistance and pyocyanin production which could also be
591 associated with this signalling molecule. Thus, we hypothesised that while Anr primarily responds
592 under anoxic conditions or severe hypoxia, other proteins, including ShrA, may regulate relevant
593 pathways under moderately-low O_2 levels after long-term exposure to hypoxia. However, we have
594 not observed any changes in the intracellular concentrations of c-di-GMP levels between the
595 ancestral early infection *P. aeruginosa* strain and any of the HACs and NACs or the late infection
596 strain despite the observed changes in related phenotypes (S6. Figure). This was not unexpected as
597 Yan et al. (2017) previously investigated the correlation between c-di-GMP levels, motility, and
598 biofilm formation (134) and did not observe any direct correlation, despite using well-established
599 models describing the mechanisms of c-di-GMP action. This finding suggests a more complex
600 regulatory network, where the final phenotypic outcome depends on the cumulative effect of

601 multiple small-scale changes rather than a straightforward 1:1 correlation. Such complexity could
602 potentially explain the seemingly contradictory observations in c-di-GMP concentrations, regulator
603 protein abundances, and variation in motility and biofilm formation.

604 Interestingly, the adaptation of *P. aeruginosa* to long-term hypoxia mirrors the phenotype
605 and molecular changes previously reported for *P. aeruginosa* chronic infection isolates
606 (8,18,21,23,36,65,68), including increased SCV prevalence, increased biofilm and exopolysaccharide
607 production, increased antibiotic resistance and decreased siderophore production. Importantly, all
608 these changes are stable, because all phenotypes were examined in normoxic conditions; thus, they
609 are a result of adaptation to hypoxia, rather than a plastic temporary response to hypoxic
610 conditions.

611 While a potential limitation of our experiment is that growth in relatively rich laboratory
612 media does not represent the conditions in the lung, the fact that we can observe changes
613 resembling adaptation to chronic infection even in the absence of nutrient stress, highlights a clear
614 role for hypoxia in this process. Choosing a planktonic model for this study allowed us to balance
615 the feasibility of the experimental design and the relevance of the model in the clinical context but
616 considering the obtained results we argue that this approach effectively reveals the potential role of
617 long-term hypoxia in driving adaptation during chronic infection.

618 Two distinct SCV types emerged in the long term cultures which were more prevalent in the
619 HACs, and one of the morphotypes was exclusive to hypoxia. We observed a temporary emergence
620 of SCV 1 in the NACs, which was not positively selected in normoxia, possibly due to the lack of an
621 adaptive benefit long-term. Under optimal laboratory conditions, long-term cultivation can induce
622 stress due to factors such as high population density, accumulation of metabolic byproducts,
623 nutrient gradients leading to transient SCV arising in the population. *P. aeruginosa* also possesses
624 phase variation systems that allow spontaneous phenotypic switching, generating SCVs even in the

625 absence of external stressors (135,136). These variants may be maintained at low frequencies,
626 preparing the population for potential environmental shifts (135). The abundance of c-di-GMP
627 signalling pathways proteins, Wsp, and YfiBNR, typically associated with SCVs (41,135), was
628 unchanged in the HACs, but as mentioned earlier, the ShrA protein indirectly regulates the Wsp
629 system activity. Additionally, the inactivation of *gacS* has been shown to be associated with the
630 emergence of SCVs under stress conditions and suppression of the reversion of this phenotype to a
631 normal colony variant (62). The latter may explain why the SCV populations in the NACs were
632 transient, as GacS is expressed in the NACs but not HACs. SCVs are strongly associated with
633 pathogenicity and persistence among several bacterial pathogens (137–139), and are prevalent
634 among chronic *P. aeruginosa* isolates (137,138,140). Specifically, SCVs of *P. aeruginosa* correlate
635 with increased exopolysaccharide and biofilm production, antimicrobial resistance, stress resistance
636 and host immune responses (41,140). Their emergence has been linked to redox imbalances which
637 can be caused by low oxygen conditions (136), although other environmental stressors or co-
638 colonisation with other species also contribute to their increased prevalence (137,140,141). This
639 confirms directly, for the first time, that prolonged hypoxia exposure is associated with increased
640 SCV occurrence in *P. aeruginosa* populations. Identification of the factors that contribute to SCV
641 emergence is crucial due to the challenges they pose in clinical settings (137) and recognising the
642 environmental factors that select this phenotype may help us limit their occurrence. Both HACs that
643 showed a high SCV prevalence (H1, H2) also showed increased resistance to a broad spectrum of
644 antimicrobials together with increased biofilm and exopolysaccharide production. Surprisingly, no
645 trends in motility relating to hypoxia exposure or biofilm formation were observed, although some
646 changes in patterns of swarming colonies were noted. Further investigation of NCVs and SCV 1 and
647 SCV 2 (genotypes and phenotypes) will provide insight on the contribution of the specific
648 subpopulations to the observed changes in other adaptations and are ongoing.

649 Chronic infection *P. aeruginosa* CF isolates typically exhibit increased biofilm and
650 exopolysaccharide production, and reduced motility (18,120,142–144), with biofilm formation
651 relying on hypoxia responses due to the presence of steep oxygen gradients (30,145,146).
652 Moreover, the awareness of the role of biofilms in antibiotic treatment efficiency is being
653 increasingly acknowledged (147,148). Proteins associated with biofilm formation, exopolysaccharide
654 production, and motility were changed in abundance. Notably, outer membrane lipoprotein PelC,
655 which is essential for biofilm formation (45), was unique to HACs while in contrast, the flagellar
656 hook protein FlgE, typically associated with motility, host interactions and immune evasion (54), was
657 absent in HACs. Both are regulated by FleQ, a c-di-GMP binding transcriptional regulator, which
658 activates the *pel* operon and inhibits the flagellar gene expression, coordinating this lifestyle switch
659 (149). Two component system regulator PilR associated with increased biofilm formation, host cell
660 attachment, and motility (58) was increased in abundance in HACs. However, the PilR-activated type
661 IV fimbrial precursor, PilA, was decreased in abundance by >13-fold in HACs compared to NACs
662 which suggests alternative regulation mechanisms are at play. Further highlighting this complexity,
663 phospholipase PlaB, showing activity towards exogenous lipids in the biofilm matrix (63), was
664 absent in HACs while UDP-glucose dehydrogenase PA3559, part of the EPS biosynthesis pathway
665 (74), was increased in abundance in HACs. These changes collectively indicate an adaptive shift
666 towards a biofilm lifestyle in HACs, aligning with changes observed in chronic infection adaptation.

667 Antibiotic resistance is a major hallmark of *P. aeruginosa* infections in CF (150), and short-
668 term hypoxic and anaerobic conditions have been previously shown to increase *P. aeruginosa*
669 antibiotic resistance (151–153). We demonstrate that long-term exposure to hypoxia induces stable
670 changes in antibiotic resistance, which importantly, didn't revert during in normoxic conditions used
671 for phenotyping. Two of the HACs showed increased resistance to a wide range of antibiotics from
672 different classes, further supporting the evidence of the extent of the influence of hypoxia pre-

673 adaptation on drug resistance and the wide range of diverse mechanisms affected. Interestingly,
674 high c-di-GMP levels have been shown to corelate with increased resistance to antibiotic,
675 independently form the biofilm/ planktonic lifestyle (128). Several proteins involved in lipid A/LPS
676 biosynthesis (LpxA, LpxB, WaaG), membrane stability (DsbG, ColR, OprH), and peptidoglycan
677 biosynthesis (MurC, PA3262), many of which have been previously linked to antibiotic resistance
678 (154–158) were altered in abundance. These may contribute to the observed broad-spectrum
679 antibiotic resistance by affecting cell envelope permeability and structure. Moreover, other proteins
680 linked to antibiotic resistance including phosphate kinase Ppk2, previously linked to multidrug
681 resistance (84), and DNA topoisomerase IV subunit ParC involved in fluoroquinolone resistance
682 (83,159) were increased in HACs (106).

683 The airways of people with CF are reported to show an increased abundance of available
684 iron (160,161). *P. aeruginosa* expresses many iron acquisition systems including siderophore
685 production, haem acquisition systems and complexes importing iron-bound citrate or catechol
686 (162). Importantly, a strong positive correlation between increased sputum iron and chronic *P.*
687 *aeruginosa* infections has been shown (163). Furthermore, iron uptake and homeostasis are
688 regulated by the c-di-GMP through the Gac/Rsm cascade (164), in line with other alterations
689 observed and underlines the role of hypoxia leading to changes in iron acquisition on chronic
690 infection development, which led to recognising them as therapy targets for *P. aeruginosa*
691 treatment (161,165). Surprisingly, we didn't observe any alterations associated with pyochelin or
692 pyoverdine biosynthesis and transport, although a clear decrease in siderophore production was
693 observed in HACs. Notably, the PchR regulator was not detected in the ancestral strain, nor in two of
694 the HACs, while present in all of the NACs, suggesting alternative mechanisms of control of
695 siderophore production or transport. Iron-sulphur cluster proteins are essential for maintaining iron
696 homeostasis and regulating diverse cellular functions (166). Notably, two iron-cluster proteins

697 frataxin-like protein CyaY, and iron-sulphur cluster scaffold protein NfuA were absent or decreased
698 in abundance in HACs, respectively. Additionally, the RhlE2 RNA helicase mentioned earlier has been
699 shown to regulate expression of iron acquisition genes. These changes may explain the decreased
700 siderophore levels observed, but require further investigation; notably, they reflect the
701 downregulation of siderophore production by chronic infection isolates from CF lungs (167).

702 Adaptation of *P. aeruginosa* to chronic infection is frequently associated with reduction in
703 expression of multiple virulence factors including pyocyanin, proteases, lipases, urease, elastase and
704 secretion systems (18). Moreover, exposure to hypoxia attenuated the virulence of isolates from
705 acute, but not chronic infections (168) and decreased their interactions with host cells,
706 demonstrating the importance of this environmental pressure. Likewise, proteomic analysis of
707 HACs, showed a decrease in abundance of many virulence factors: proteases (PasP serine protease,
708 aminopeptidase PepA, aminopeptidase PepN), Phospholipase B, and type VI secretion system
709 (TssB1, Tse8 effector protein) and type II secretion system effector proteins (PasP, PilA). LasI, a
710 component of the QS system was not detected in HACs or the ancestral strain, but present in NACs.
711 Since it positively regulates protease and lipase synthesis (and indirectly T6SS), its decreased
712 abundance is consistent with the other alterations. Interestingly, phenazine biosynthesis protein
713 PhzE was unique to HACs, which would suggest an increase in pyocyanin production in all HACs,
714 however, we detected a change in pyocyanin in only two cultures. Thus, we might have expected
715 decreased virulence in HACs, but did not observe any change in the *G. mellonella* infection model
716 following hypoxia exposure. However, this acute infection model may not be optimal to assess the
717 impact of long-term hypoxia adaptation on chronic infection.

718 Some of the observed changes in phenotypes, including increased biofilm and EPS
719 production, and antibiotic resistance may result from the increased prevalence of the SCVs in the
720 population, as all of these are altered in HAC 1 and 2, while limited changes were observed in HAC

721 3. Investigation of this is ongoing, however, given that many alterations in the proteome were
722 conserved across all three HACs, despite divergent phenotypic outcomes suggests a more complex
723 explanation involving additional, SCV-independent adaptive mechanisms.

724 A recent study defined *P. aeruginosa* 224 genes as pathoadaptive, and demonstrated that
725 specific gene expression was associated with a host preference towards people with CF (169), many
726 of which encode proteins altered in response to long-term hypoxia. Three of these, ColR, GacS and
727 MexS were not detected in HACs, while another, PA0664 protein was maintained in HACs while not
728 detected in NACs. Additionally, PilR and ParC were increased in abundance in HACs respectively,
729 while OprM was decreased in abundance. Moreover, overall changes in the abundance of 15
730 proteins encoded by genes that were associated with CF host preference (including *oprM*, *pepA*,
731 *fimV*, and *pilR*) and 11 that were associated with non-CF infections (including *mvaT* and *tssB1*) (169),
732 suggest long-term hypoxia may play a role in *P. aeruginosa* infection both in CF and non-CF cohorts.

733

734 Common adaptation mechanisms of opportunistic pathogens to hypoxia

735 Several oxygen-sensing mechanisms, homologous genes in hypoxia regulons and several
736 phenotypes altered in chronic infection are shared across other opportunistic bacteria causing
737 pulmonary infections. This suggests that adaptation to prolonged hypoxia could be a shared
738 mechanism between many low oxygen and/or microaerophilic habitats and not limited to human
739 infections. These environments are increasingly abundant in water and soil, where opportunistic
740 bacteria reservoirs exist, and play significant roles in shaping their physiology, contributing to their
741 increased prevalence (170–174). As many opportunistic bacterial pathogens causing CF infections
742 reside in these niches, common adaptations are not unexpected.

743 Proteome analysis of HACs showed an increase in abundance of only two proteins encoded
744 on the Anr regulon (113), the Ppk2 and the AdhA alcohol dehydrogenase while NorC was not
745 detected in HACs but present in NACs and the ancestral strain. Only three proteins from the Anr
746 core regulon being altered is surprising, since hypoxia response has been primarily associated with
747 it. However, as previously mentioned, Anr regulation is complex, and hypoxia adaptation may have
748 selected for strains that downregulate Anr to conserve energy. Additionally, as mentioned the
749 moderate hypoxic conditions utilised may lead to adaptation via other pathways rather than the Anr
750 regulon. Notably, the Anr regulon shares homologous genes with the DosR regulon of
751 *Mycobacterium abscessus* and Lxa locus of *Burkholderia cenocepacia*, highlighting that aspects of
752 the hypoxia response may be shared across several opportunistic CF lung infections more generally.
753 Investigations on the impact of different levels of hypoxia on these three pathogens is ongoing in
754 our group. Targeting shared mechanisms of adaptation to chronic infection could present a new
755 opportunity for the treatment of multiple pathogens simultaneously.

756

757 **Impact**

758 Overall, we demonstrate that alterations in phenotype after long-term exposure to hypoxic
759 conditions shows several similarities associated with chronic infection. Further understanding of the
760 mechanisms by which *P. aeruginosa* adapts to hypoxia in chronic infection and the interplay with
761 other factors present in the lung environment will potentially enable us to prevent or treat the
762 switch from acute to chronic infection. This could inevitably limit antibiotic use, severity of the
763 disease and ultimately, decrease the socioeconomic impact of infections caused by *P. aeruginosa*.
764 Furthermore, the first drug to alter the human response to hypoxia was recently approved for use
765 by the US Food and Drug Administration (175). Thus, it is tempting to speculate that the response of

766 bacteria to low oxygen pressures could be targeted to prevent a switch from acute to chronic
767 infection.

768 The observed changes in proteome and phenotypes (increased biofilm formation, increased
769 antibiotic resistance, decreased siderophore production, increased SCV prevalence) further deepens
770 our knowledge on how hypoxia leads to adaptation of *P. aeruginosa*, shedding light on how
771 prolonged low oxygen exposure can impact on adaptation to chronic infection. Overall, we confirm
772 that hypoxia contributes to the development of multiple phenotypic changes that are prevalent in
773 chronic infection, opening a path towards designing therapies targeting these.

774

775

776

777

778

779

780 Materials and methods

781 Bacterial strains

782 *Pseudomonas aeruginosa* AMT 0023-30 early infection clinical strain (E) and AMT 0023-34 late
783 infection clinical strain (L) are two well characterised strains in the International *P. aeruginosa* panel
784 (35). Hypoxia- and normoxia-adapted *P. aeruginosa* strains were obtained in this study as described
785 below and are referred to as H1, H2, H3, N1, N2, and N3 (Table 1). If not stated otherwise, bacteria

786 were routinely grown in LB broth (Sigma-Aldrich, St. Louis, MO, USA) at 37°C with orbital agitation
787 (200 rpm) or plated on LB agar (Sigma-Aldrich, St. Louis, MO, USA) and grown at 37°C.

788 Experimental evolution

789 Overnight cultures of *P. aeruginosa* strain AMT 0023-30 (E) were inoculated into 30 ml LB media to
790 OD_{600} ~0.1. Prior to use, the media was equilibrated for 18 h at 37°C in an O_2 Control InVitro Glove
791 Box (PHGB model, Coy Laboratory Products, MI, United States) at 6% O_2, 5% CO_2 or in a Steri-Cycle
792 CO_2 Incubator (model 371, Thermo Scientific, Waltham, MA, USA) at 21% O_2, 5% CO_2. Three flasks
793 were inoculated as biological replicates for each of the conditions being examined. Additionally,
794 aliquots (2 ml) of the overnight *P. aeruginosa* cultures were retained as a control for proteomic and
795 transcriptomic analysis. All flasks were incubated for 24h with agitation (200 rpm, CO_2 resistant
796 orbital shaker, model 15351105, Thermo Fisher Scientific, Waltham, MA, USA) in hypoxic and
797 normoxic conditions. Daily aliquots (2 ml) were removed for proteomic analysis from each of the
798 flasks and also additional aliquots retained for OD_{600} measurements and plating. Glycerol stocks
799 (50%, LB (v/v)) were prepared for subsequent phenotype analysis and frozen immediately to ensure
800 minimal oxygen exposure. A volume of 5% of the bacterial culture was also transferred into 30 ml of
801 pre-equilibrated media each day and this procedure was continued for up to 28 days to determine
802 long-term adaptation patterns. To ensure stability of the hypoxic conditions, all of the samples from
803 H1, H2 and H3 were taken inside the hypoxia chamber. To ensure that there were no other
804 environmental differences between the test conditions other than oxygen levels, the same batch of
805 media was used for both normoxia-adapting and hypoxia-adapting flasks and shaking conditions
806 were consistently maintained.

807 Whole proteome analysis

808 Samples (2 ml) were collected throughout the experimental evolution for proteome analysis.
809 Bacterial cells were pelleted at 14000-16000 g for 2 min and stored at -80°C until further analysis.
810 Whole cell lysates were extracted from each of the hypoxia- and normoxia exposed cultures by
811 resuspending in 1 ml of ice-cold lysis buffer containing 40mM Tris-HCl (pH 7.8) and 1x cOmplete™,
812 EDTA-free protease inhibitor cocktail (Roche, Basel, Switzerland). Cells were disrupted by a
813 sonication with a sonic dismembrator and microtip 6mm probe (model 505; Fisherbrand, Thermo
814 Fisher Scientific, Waltham, MA, USA) (set with 20% output power using eight 10 s bursts on ice). Cell
815 debris and any remaining intact cells were pelleted using centrifugation (12000 g for 30 min).
816 Supernatants were transferred into fresh tubes and the proteins were precipitated with four
817 volumes of methanol and incubated in -80°C overnight. The samples were centrifuged at 12000 g
818 for 30 min at 4°C, supernatants were removed, and the protein pellets were resuspended in 200 µl
819 of resuspension buffer containing 8 M urea, 50 mM Tris-HCL (pH 8.0), before 1 M 1,4-dithiothreitol
820 (DTT) was added to each supernatant (10 µl/ml lysate) and incubated at 56°C for 30 min, followed
821 by the addition of 1 M iodoacetamide (55 µl/ml lysate) which was incubated in darkness at room
822 temperature for 20 min. Lysates were dialyzed in SnakeSkin™ tubing (Thermo Fisher Scientific,
823 Waltham, MA, USA) with a cut-off of 3.5 kDa against 100 mM ammonium bicarbonate overnight,
824 with stirring at 4°C, followed by at least 4 more hours incubation with fresh volumes of ammonium
825 bicarbonate. Trypsin (400 ng/µl) (Sigma-Aldrich, St. Louis, MO, USA) was added to the dialyzed
826 protein (5 µl /100 µl protein) and tubes were incubated overnight at 37°C. Aliquots from each
827 sample were placed in fresh tubes and samples were dried in a vacufuge concentrator system
828 (model 5301; Eppendorf, Hamburg, Germany) at 65°C and resuspended in 20 µl of ZipTips
829 resuspension buffer containing 0.5% trifluoroacetic acid (TFA) in MilliQ water. ZipTips (Merc
830 Millipore, Burlington, MA, USA) were used for peptide purification as per the manufacturers'
831 instructions. Nanodrop spectrophotometer DS-11+ (DeNovix, Wilmington, DE, USA) was used for
832 peptide concentration measurements. The samples were analysed on a Bruker TimsTOF Pro mass

833 spectrometer connected to a Evosep One chromatography system. Peptides were separated on an
834 8 cm analytical C18 column (Evosep, 3 µm beads, 100 µm ID) using the pre-set 33 samples per day
835 gradient on the Evosep one. A trapped ion mobility (TIMS) analyser was synchronized with a
836 quadrupole mass filter to enable the highly efficient PASEF (Parallel Accumulation Serial
837 Fragmentation acquisition) procedure with acquisition rates of 100 Hz. The accumulation and ramp
838 times for the TIMS were both set to 100 ms., with an ion mobility (1/k0) range from 0.62 to 1.46
839 Vs/cm. Spectra were recorded in the mass range from 100 to 1,700 m/z. The precursor (MS)
840 Intensity Threshold was set to 2,500 and the precursor Target Intensity set to 20,000. Each PASEF
841 cycle consisted of one MS ramp for precursor detection followed by 10 PASEF MS/MS ramps, with a
842 total cycle time of 1.16 s.

843 Protein identification and label-free quantitative (LFQ) analysis were conducted using MaxQuant (v
844 2.4.2.0, https://maxquant.org/) by searching against the reference strain *P. aeruginosa* PAO1 (ATCC
845 15692). For protein identification, the following search parameters were used: trypsin was the
846 digesting enzyme with up to two missed cleavages allowed for; oxidation on methionine and
847 acetylation on the N terminus were selected as variable modifications with a fixed modification of
848 carbamidylation on cysteine; Label Free Quantitation (LFQ) and Match Between Runs (MBR) options
849 were selected. FDR for protein and peptide were set at 1%.

850 The three biological replicates from each 28 day culture condition were analysed, with one technical
851 replicate for a randomly chosen sample and LFQ intensities were compared. All missing LFQ
852 intensities were imputed with a fixed value of 1. The mean was calculated separately for the hypoxia
853 and normoxia samples, followed by fold change (FC) calculation.

854 One-way ANOVA statistical analysis (p-value ≤0.05) together with Benjamini–Hochberg false-
855 discovery adjustment were performed to identify proteins with a significantly changed abundance
856 Proteins with adjusted p-values≤0.1 were considered significantly altered in abundance.

857 Functional enrichment of proteins significantly changed in abundance was performed. For GO
858 biological process functional enrichment analysis ShinyGO (v 0.82) (44) was used. Species was set to
859 *P. aeruginosa* PAO1, FDR cutoff was set to 0.05 and the minimal pathway size was set as two. For
860 STRING local network and KEGG pathway enrichment the STRING (v 12.0) database was used with
861 default settings.

862 Antibiotic resistance

863 Overnight bacterial cultures were diluted in 10 ml of fresh LB to OD_{600} equal to 0.1. Bacteria were
864 spread evenly on Mueller–Hinton agar plates (Neogen, Lansing, MI, USA) using cotton swabs, in
865 three directions, to give a homogenous lawn. Antibiotic disks (Oxoid, Hampshire, UK) were placed
866 on the surface of the agar and the plates were incubated overnight in normoxic conditions at
867 37°C. Growth inhibition zone diameters were measured in at least two points, and the mean was
868 used for statistical analysis. The experiment was repeated three times. The following antibiotics
869 were tested: norfloxacin (10 µg), ciprofloxacin (10 µg), azithromycin (15 µg), clarithromycin (15 µg),
870 ceftazidime (30 µg), meropenem (10 µg), imipenem (10 µg), piperacillin (100 µg), aztreonam (30
871 µg), tobramycin (10 µg), and tetracycline (30 µg).

872

873

874 Motility

875 Motility assays were performed as described previously (176). Swimming motility was assessed by
876 inoculating the surface of a 0.3 % (w/v) LB agar plate with overnight culture using a sterile
877 toothpick. Swimming and swarming plates were incubated overnight in normoxic conditions at 37°C
878 for ~18 h. For swarming motility 0.8% nutrient broth (Sigma-Aldrich, St. Louis, MO, USA), 0.5%

879 dextrose, 0.5% agar plates were inoculated identically as for swimming motility assessment. The
880 diameter of bacterial growth zones was measured in at least two directions, and the mean was used
881 for statistical analysis. Twitching motility was assessed by inoculating 1.5 % (w/v) LB agar plate by
882 piercing through the agar. Plates were incubated overnight in normoxic conditions at 37°C for ~18 h,
883 and the agar was removed. Bacteria on the surface of the plate were stained with 1% (w/v) crystal
884 violet for 20 min. The plates were washed with water until all excess dye was removed and dried at
885 room temperature. The diameter of the growth zone was measured in at least two points, and the
886 mean was used for statistical analysis. The experiment was repeated three times.

887 Biofilm production

888 Overnight cultures of *P. aeruginosa* strains were diluted in fresh LB media to OD_{600} of ~0.1, and
889 100 µl of each diluted culture was transferred into 6 wells of a 96-well plate. The plates were
890 incubated statically in normoxic conditions at 37°C for 24, 48 or 72 h and OD_{600} was measured with
891 the Synergy H1 microplate reader (Mason Technology, Dublin, Ireland). The medium with planktonic
892 bacteria was removed, and the biofilm fixed by incubation with 200ul of methanol for 10 min. The
893 wells were washed three times with phosphate buffered saline (PBS) (Sigma-Aldrich, St. Louis, MO,
894 USA), followed by the addition of 200 µl of 0.1% crystal violet solution and 30 min incubation at
895 room temperature. The solution was removed, and the wells were washed three times with water
896 and once with PBS. The plates were dried for at least 30 min at room temperature and 150 µl of
897 96% ethanol was added to dissolve the bound stain. After 10 min of incubation at room
898 temperature, the solution was mixed by pipetting, OD_{590} was determined, and the OD_{590}/OD_{600} ratio
899 was calculated. The experiment was repeated three times.

900 Exopolysaccharide production - Congo Red agar assay

901 Overnight cultures of *P. aeruginosa* strains were pelleted and washed with 1 ml of PBS. The pellets
902 were resuspended in PBS to OD_{600} of ~0.1 and 1 µl of the suspension was plated on a Congo Red
903 agar plate (10 g/L Tryptone, 10 g/ L Bactoagar, 40mg/L Congo Red, 20mg/L Coomassie Brilliant
904 Blue). The plates were incubated for 48 h in normoxic conditions and colony morphology was
905 assessed. The experiment was repeated three times.

906 Stress sensitivity assays

907 Overnight cultures of *P. aeruginosa* strains were diluted to a CFU/ml of 10^8 and a range of serial
908 dilutions was prepared. Suspensions (1µl) were plated on one of the following: LB agar control
909 plates, LB agar supplemented with 0.5 M NaCl (osmotic stress), LB agar supplemented with 1mM
910 H_2O_2 (oxidative stress), or LB agar, pH 5 (acidic stress). The plates were incubated in normoxic
911 conditions at 37°C for 24 or 48 h. Temperature stress was determined by incubation of an LB agar
912 plate at 45°C for 24 h. Change of sensitivity was determined by determining the lowest dilution at
913 which bacterial growth was observed. The experiment was repeated three independent times.

914 *Galleria mellonella* infection model

915 Virulence was determined as previously described (37). Wax moth larvae (*Galleria mellonella*) (The
916 KammieShop, Waalwijk, Denmark) were equilibrated in normoxic conditions at 15°C for at least 7
917 days after arrival and stored at the same conditions for up to 4 weeks, during which larvae with a
918 weight range of 0.2-0.4 g were selected for experiments. Overnight bacterial cultures in LB were
919 diluted in fresh media to OD_{600} of ~0.1 and grown for 2-3 h. Cultures were centrifuged, and
920 bacterial cells were washed with PBS. The bacteria were diluted to 10^6 CFU/ml and serially diluted
921 to 10^{-6}. Each dilution was injected (20 µl) into the hindmost left proleg of healthy larvae (10 per
922 group) and the same volume of PBS was injected into one group as a control. Injected larvae were
923 incubated at 37°C for 72 h. To have an accurate count of the bioburden inoculated, aliquots of the

924 bacteria injected were serially diluted and plated onto LB agar and colonies counted after 24 h. The
925 experiment was repeated at least three times for each strain tested.

926 Pyocyanin production quantification

927 *P. aeruginosa* strains were inoculated to OD_{600} in fresh PB media (20g/L Bacto-Peptone, 1.4g/L
928 $MgCl_2$, 10g/L K_2SO_4) and cultured with aeration in normoxic conditions at 37°C to maximize
929 pyocyanin production. The bacterial cultures were pelleted (10 min at 12300 g) and two 7.5-ml
930 replicates were withdrawn from each of the 18 h stationary phase cultures. Pyocyanin was extracted
931 with 4.5 ml of chloroform and a total of 1.5 ml of 0.2 M HCl was added to each extract causing
932 colour change from blue to pink. The absorbance of this solution was measured at 520 nm, and the
933 obtained values were converted to pyocyanin content following Essar et al. (1990) (48). The
934 experiment was repeated at least two times.

935 Siderophore production

936 The siderophore production was quantified with a modified version of a microplate method
937 developed previously (177). Prior to siderophore quantification all glassware was rinsed with a 3M
938 solution of HCl to remove trace iron and rinsed thoroughly with deionised water. The CAS reagent
939 was prepared as described before (177).

940 Three independent cultures of each tested population or strain were grown in fresh LB medium for
941 48 h at 37°C with agitation in normoxic conditions. Aliquots of the cultures were taken for CFU
942 counts, serially diluted and plated on LB agar. The cultures were spun down (10 min at 12300 g), and
943 50 µl aliquots of the supernatant were transferred into separate wells of a microplate followed by
944 an immediate addition of 100 µl of CAS reagent. As a control LB broth was used. The plates were
945 incubated for 20 min at room temperature in the dark and the optical density was measured at 630

946 nm using the Synergy H1 microplate reader. The Siderophore units were calculated as follows:
947 siderophore production = $[(A_{LB} - A_s) * 100]/A_{LB}$, where A_{LB} = absorbance of LB control and A_s =
948 absorbance of sample. The earlier plated bacteria were incubated at 37°C overnight and colony
949 forming units were counted. Siderophore production per colony forming unit was calculated to
950 account for any differences in growth. The experiment was repeated two times.

951 Determination of growth by optical density

952 To assess the influence of the inoculation volume on the growth patterns of *P. aeruginosa* AMT
953 0023-30, 24h stationary phase cultures were inoculated into fresh LB media in a way they
954 constituted 1%, 5% or 10% of the new culture. Three 200 µl technical replicates of the cultures were
955 transferred into a 96-well plate and incubated in the Synergy H1 microplate reader in normoxic
956 conditions at 37°C with agitation with OD_{600} measurements taken every 30 min.

957 Determination of growth by CFU

958 To assess the differences in the numbers of generations in hypoxic conditions and normoxic
959 conditions of the AMT0063-30 early infection strain overnight cultures were prepared. The
960 following day they were inoculated in triplicate into fresh LB media and incubated with aeration at
961 37°C in the O_2 Control InVitro Glove Box in 6% O_2, 5% CO_2 or in 21% O_2, 5% CO_2 or in the Steri-Cycle
962 CO_2 Incubator at 21% O_2, 5% CO_2. Every hour a sample was taken from each culture for OD_{600}
963 measurements and plating on LB agar. The agar plates were incubated overnight at 37°C and the
964 colony forming units were calculated and OD_{600} to CFU/ml was plotted, a trend line was determined
965 and R^2 calculated. The doubling time was calculated for the logarithmic phase of growth using the
966 following formula: Doubling time = (Duration (min)*ln(2))/[ln(final cell concentration/initial cell
967 concentration)].

968 ## Intracellular c-di-GMP concentration measurements:

969 C-di-GMP was extracted from *P. aeruginosa* cells as previously described (178). Briefly, the OD_{600} of
970 overnight cultures was measured, and a culture volumes equivalent to 4 ml of OD_{600} = 1.8 were
971 centrifuged and washed twice with PBS. Pellets were resuspended in 400 µl PBS, incubated at
972 100°C for 5 min before adding ice-cold ethanol (final concentration of 65%), and mixing. The
973 supernatants were collected after centrifugation and the extraction was repeated three times.
974 Pooled supernatants were dried at 30°C, resuspended in 200 µl nanopure water, and c-di-GMP
975 levels were quantified using a cyclic-di-GMP assay kit (Lucerna Technologies, Brooklyn, NY, USA), as
976 per the manufacturer's recommendations. C-di-GMP concentrations were normalized to total
977 protein content, measured using the Bradford reagent (Sigma-Aldrich, St. Louis, MO, USA) on pellets
978 that were resuspended in TE buffer, sonicated on ice for 1 min (10 s bursts, 20% output power),
979 centrifuged and the supernatants used for protein quantification.

980 ## Statistical analysis of phenotype data

981 Initial data preparation was performed using Microsoft Excel and statistical analysis was performed
982 using GraphPad Prism (v 8.0.2, GraphPad Software, Boston, MA, US). Only p-values of 0.05 or lower
983 were considered statistically significant. First, the normality was assessed using the Shapiro-Wilk
984 test. Data with normal distribution was analysed using the Ordinary one-way ANOVA with the
985 Uncorrected Fisher's LSD; data with non-normal distribution was analysed using the Kruskal-Wallis
986 test with an uncorrected Dunn's test. Details of the analysis and significance are provided in figure
987 legends.

988 # Acknowledgements

JD, CJC are supported by an SFI Frontiers of the Future award (20/FFP-P/8717) to SMcC. ND was supported by the Irish Research Council, GOIPG/2021/1443 IRC Award. The authors are grateful to Dr David Gomez-Matallanas for his advice in proteomic analysis and for the support of the staff and facilities in the UCD Conway proteomics core.

References

1. Antimicrobial resistance collaborators. Antimicrobial Resistance Collaborators: Global burden of bacterial antimicrobial resistance in 2019: a systematic analysis. Lancet. 2022 Feb 12;399(10325):629–55.
2. O'Neill J. Tackling drug-resistant infections globally: final report and recommendations. Wellcome Trust; 2016.
3. Blanchard AC, Waters VJ. Opportunistic Pathogens in Cystic Fibrosis: Epidemiology and Pathogenesis of Lung Infection. Journal of the Pediatric Infectious Diseases Society. 2022 Sep 1;11(Supplement_2):S3–12.
4. Sanz-García F, Gil-Gil T, Laborda P, Ochoa-Sánchez LE, Martínez JL, Hernando-Amado S. Coming from the Wild: Multidrug Resistant Opportunistic Pathogens Presenting a Primary, Not Human-Linked, Environmental Habitat. International Journal of Molecular Sciences. 2021 Jan;22(15):8080.
5. Serra-Burriel M, Keys M, Campillo-Artero C, Agodi A, Barchitta M, Gikas A, et al. Impact of multi-drug resistant bacteria on economic and clinical outcomes of healthcare-associated infections in adults: Systematic review and meta-analysis. PLoS One. 2020;15(1):e0227139.
6. Reynolds D, Kollef M. The Epidemiology and Pathogenesis and Treatment of Pseudomonas aeruginosa Infections: An Update. Drugs. 2021 Dec 1;81(18):2117–31.
7. Li Y, Roberts JA, Walker MM, Aslan AT, Harris PNA, Sime FB. The global epidemiology of ventilator-associated pneumonia caused by multi-drug resistant *Pseudomonas aeruginosa*: A systematic review and meta-analysis. International Journal of Infectious Diseases. 2024 Feb 1;139:78–85.
8. Rossi E, La Rosa R, Bartell JA, Marvig RL, Haagensen JAJ, Sommer LM, et al. Pseudomonas aeruginosa adaptation and evolution in patients with cystic fibrosis. Nat Rev Microbiol. 2021 May;19(5):331–42.
9. Smith WD, Bardin E, Cameron L, Edmondson CL, Farrant KV, Martin I, et al. Current and future therapies for Pseudomonas aeruginosa infection in patients with cystic fibrosis. FEMS Microbiology Letters. 2017 Aug 1;364(14):fnx121.
10. Botelho J, Grosso F, Peixe L. Antibiotic resistance in *Pseudomonas aeruginosa* – Mechanisms, epidemiology and evolution. Drug Resistance Updates. 2019 May 1;44:100640.
11. Bakkeren E, Diard M, Hardt WD. Evolutionary causes and consequences of bacterial antibiotic persistence. Nat Rev Microbiol. 2020 Sep;18(9):479–90.
12. Sett A, Dubey V, Bhowmik S, Pathania R. Decoding Bacterial Persistence: Mechanisms and Strategies for Effective Eradication. ACS Infect Dis. 2024 Aug;
13. ECDC. Healthcare-associated infections acquired in intensive care units - Annual Epidemiological Report for 2016. Stockholm; 2018.

1029 14. ECDC. Healthcare-associated infections acquired in intensive care units - Annual
1030 Epidemiological Report for 2019. Stockholm; 2023.
1031 15. Tacconelli E, Carrara E, Savoldi A, Harbarth S, Mendelson M, Monnet DL, et al. Discovery,
1032 research, and development of new antibiotics: the WHO priority list of antibiotic-resistant
1033 bacteria and tuberculosis. The Lancet Infectious Diseases. 2018 Mar 1;18(3):318–27.
1034 16. WHO. WHO bacterial priority pathogens list, 2024: Bacterial pathogens of public health
1035 importance to guide research, development and strategies to prevent and control
1036 antimicrobial resistance. 2024.
1037 17. Cullen L, McClean S. Bacterial Adaptation during Chronic Respiratory Infections. Pathogens.
1038 2015 Mar;4(1):66–89.
1039 18. Jurado-Martín I, Sainz-Mejías M, McClean S. Pseudomonas aeruginosa: An Audacious
1040 Pathogen with an Adaptable Arsenal of Virulence Factors. Int J Mol Sci. 2021 Mar
1041 18;22(6):3128.
1042 19. Camus L, Vandenesch F, Moreau K. From genotype to phenotype: adaptations of Pseudomonas
1043 aeruginosa to the cystic fibrosis environment. Microbial Genomics. 2021;7(3):000513.
1044 20. Chadha J, Harjai K, Chhibber S. Revisiting the virulence hallmarks of Pseudomonas aeruginosa:
1045 a chronicle through the perspective of quorum sensing. Environmental Microbiology.
1046 2022;24(6):2630–56.
1047 21. Cramer N, Klockgether J, Tümmler B. Microevolution of Pseudomonas aeruginosa in the
1048 airways of people with cystic fibrosis. Current Opinion in Immunology. 2023 Aug 1;83:102328.
1049 22. Moradali MF, Ghods S, Rehm BHA. Pseudomonas aeruginosa Lifestyle: A Paradigm for
1050 Adaptation, Survival, and Persistence. Front Cell Infect Microbiol. 2017 Feb 15;7(39).
1051 23. Rosales-Reyes R, Vargas-Roldán SY, Lezana-Fernández JL, Santos-Preciado JI. *Pseudomonas*
1052 *Aeruginosa*: Genetic Adaptation, A Strategy for its Persistence in Cystic Fibrosis. Archives of
1053 Medical Research. 2021 May 1;52(4):357–61.
1054 24. Feng Q, Zhou J, Zhang L, Fu Y, Yang L. Insights into the molecular basis of c-di-GMP signalling in
1055 Pseudomonas aeruginosa. Critical Reviews in Microbiology. 2024 Jan 2;50(1):20–38.
1056 25. Krasteva PV, Giglio KM, Sondermann H. Sensing the messenger: The diverse ways that bacteria
1057 signal through c-di-GMP. Protein Science. 2012;21(7):929–48.
1058 26. Valentini M, Filloux A. Multiple Roles of c-di-GMP Signaling in Bacterial Pathogenesis. Annual
1059 Review of Microbiology. 2019 Sep 8;73(Volume 73, 2019):387–406.
1060 27. Hall CL, Lee VT. Cyclic-di-GMP regulation of virulence in bacterial pathogens. WIREs RNA.
1061 2018;9(1):e1454.
1062 28. Worlitzsch D, Tarran R, Ulrich M, Schwab U, Cekici A, Meyer KC, et al. Effects of reduced mucus
1063 oxygen concentration in airway Pseudomonas infections of cystic fibrosis patients. J Clin Invest.
1064 2002 Feb;109(3):317–25.
1065 29. Alvarez-Ortega C, Harwood CS. Responses of Pseudomonas aeruginosa to low oxygen indicate
1066 that growth in the cystic fibrosis lung is by aerobic respiration. Molecular Microbiology.
1067 2007;65(1):153–65.
1068 30. Hassett DJ, Sutton MD, Schurr MJ, Herr AB, Caldwell CC, Matu JO. Pseudomonas aeruginosa
1069 hypoxic or anaerobic biofilm infections within cystic fibrosis airways. Trends in Microbiology.
1070 2009 Mar 1;17(3):130–8.
1071 31. Cullen L, O'Connor A, McCormack S, Owens RA, Holt GS, Collins C, et al. The involvement of the
1072 low-oxygen-activated locus of Burkholderia cenocepacia in adaptation during cystic fibrosis
1073 infection. Sci Rep. 2018 Sep 6;8(1):13386.

1074 32. O'Connor A, Jurado-Martín I, Mysior MM, Manzira AL, Drabinska J, Simpson JC, et al. A
1075 universal stress protein upregulated by hypoxia has a role in Burkholderia cenocepacia
1076 intramacrophage survival: Implications for chronic infection in cystic fibrosis.
1077 Microbiologyopen. 2022 Dec 9;12(1):e1311.
1078 33. Cullen L, O'Connor A, Drevinek P, Schaffer K, McClean S. Sequential Burkholderia cenocepacia
1079 Isolates from Siblings with Cystic Fibrosis Show Increased Lung Cell Attachment. Am J Respir
1080 Crit Care Med. 2017 Mar 15;195(6):832–5.
1081 34. Cao P, Fleming D, Moustafa DA, Dolan SK, Szymanik KH, Redman WK, et al. A Pseudomonas
1082 aeruginosa small RNA regulates chronic and acute infection. Nature. 2023 Jun;618(7964):358–
1083 64.
1084 35. De Soyza A, Hall AJ, Mahenthiralingam E, Drevinek P, Kaca W, Drulis-Kawa Z, et al. Developing
1085 an international Pseudomonas aeruginosa reference panel. Microbiologyopen. 2013
1086 Dec;2(6):1010–23.
1087 36. Freschi L, Bertelli C, Jeukens J, Moore MP, Kukavica-Ibrulj I, Emond-Rheault JG, et al. Genomic
1088 characterisation of an international Pseudomonas aeruginosa reference panel indicates that
1089 the two major groups draw upon distinct mobile gene pools. FEMS Microbiol Lett. 2018 Jul
1090 1;365(14).
1091 37. Cullen L, Weiser R, Olszak T, Maldonado RF, Moreira AS, Slachmuylders L, et al. Phenotypic
1092 characterization of an international Pseudomonas aeruginosa reference panel: strains of cystic
1093 fibrosis (CF) origin show less in vivo virulence than non-CF strains. Microbiology.
1094 2015;161(10):1961–77.
1095 38. Mulcahy LR, Burns JL, Lory S, Lewis K. Emergence of Pseudomonas aeruginosa Strains
1096 Producing High Levels of Persister Cells in Patients with Cystic Fibrosis. Journal of Bacteriology.
1097 2010 Oct 8;192(23):6191.
1098 39. Aanaes K, Rickelt LF, Johansen HK, von Buchwald C, Pressler T, Høiby N, et al. Decreased
1099 mucosal oxygen tension in the maxillary sinuses in patients with cystic fibrosis. J Cyst Fibros.
1100 2011 Mar;10(2):114–20.
1101 40. Walkiewicz A, Brzezińska M, Bieganowski A. Methanotrophs are favored under hypoxia in
1102 ammonium-fertilized soils. Biol Fertil Soils. 2018 Oct 1;54(7):861–70.
1103 41. Xu A, Zhang X, Wang T, Xin F, Ma LZ, Zhou J, et al. Rugose small colony variant and its hyper-
1104 biofilm in *Pseudomonas aeruginosa*: Adaption, evolution, and biotechnological potential.
1105 Biotechnology Advances. 2021 Dec 1;53:107862.
1106 42. The Galaxy Community. The Galaxy platform for accessible, reproducible, and collaborative
1107 data analyses: 2024 update. Nucleic Acids Research. 2024 Jul 5;52(W1):W83–94.
1108 43. Szklarczyk D, Kirsch R, Koutrouli M, Nastou K, Mehryary F, Hachilif R, et al. The STRING
1109 database in 2023: protein-protein association networks and functional enrichment analyses for
1110 any sequenced genome of interest. Nucleic Acids Res. 2023 Jan 6;51(D1):D638–46.
1111 44. Ge SX, Jung D, Yao R. ShinyGO: a graphical gene-set enrichment tool for animals and plants.
1112 Bioinformatics. 2020 Apr 15;36(8):2628–9.
1113 45. Marmont LS, Rich JD, Whitney JC, Whitfield GB, Almblad H, Robinson H, et al. Oligomeric
1114 lipoprotein PelC guides Pel polysaccharide export across the outer membrane of Pseudomonas
1115 aeruginosa. Proceedings of the National Academy of Sciences. 2017 Mar 14;114(11):2892–7.
1116 46. Culbertson JE, Toney MD. Expression and characterization of PhzE from *P. aeruginosa* PAO1:
1117 aminodeoxyisochorismate synthase involved in pyocyanin and phenazine-1-carboxylate
1118 production. Biochimica et Biophysica Acta (BBA) - Proteins and Proteomics. 2013 Jan
1119 1;1834(1):240–6.

1120 47. Wang Y, Wang L, Zhang J, Duan X, Feng Y, Wang S, et al. PA0335, a Gene Encoding Histidinol
1121 Phosphate Phosphatase, Mediates Histidine Auxotrophy in Pseudomonas aeruginosa. Applied
1122 and Environmental Microbiology. 2020 Feb 18;86(5):e02593-19.
1123 48. Essar DW, Eberly L, Hadero A, Crawford IP. Identification and characterization of genes for a
1124 second anthranilate synthase in Pseudomonas aeruginosa: interchangeability of the two
1125 anthranilate synthases and evolutionary implications. J Bacteriol. 1990 Feb;172(2):884–900.
1126 49. Rojas Murcia N, Lee X, Waridel P, Maspoli A, Imker HJ, Chai T, et al. The Pseudomonas
1127 aeruginosa antimetabolite L -2-amino-4-methoxy-trans-3-butenoic acid (AMB) is made from
1128 glutamate and two alanine residues via a thiotemplate-linked tripeptide precursor. Front
1129 Microbiol [Internet]. 2015 Mar 12 [cited 2025 Jun 27];6. Available from:
1130 https://www.frontiersin.org/journals/microbiology/articles/10.3389/fmicb.2015.00170/full
1131 50. Müsken M, Di Fiore S, Dötsch A, Fischer R, Häussler S. Genetic determinants of Pseudomonas
1132 aeruginosa biofilm establishment. Microbiology (Reading). 2010 Feb;156(Pt 2):431–41.
1133 51. Smith EW, Zhang X, Behzadi C, Andrews LD, Cohen F, Chen Y. Structures of Pseudomonas
1134 aeruginosa LpxA Reveal the Basis for Its Substrate Selectivity. Biochemistry. 2015 Sep
1135 29;54(38):5937–48.
1136 52. Hou M, Huang J, Jia T, Guan Y, Yang F, Zhou H, et al. Deep Profiling of the Proteome Dynamics
1137 of Pseudomonas aeruginosa Reference Strain PAO1 under Different Growth Conditions. J
1138 Proteome Res. 2023 Jun 2;22(6):1747–61.
1139 53. Florek LC, Lin X, Lin YC, Lin MH, Chakraborty A, Price-Whelan A, et al. The L-lactate
1140 dehydrogenases of Pseudomonas aeruginosa are conditionally regulated but both contribute
1141 to survival during macrophage infection. mBio. 2024 Aug 20;15(9):e00852-24.
1142 54. You Y, Ye F, Mao W, Yang H, Lai J, Deng S. An overview of the structure and function of the
1143 flagellar hook FlgE protein. World J Microbiol Biotechnol. 2023 Mar 21;39(5):126.
1144 55. Valentin JDP, Straub H, Pietsch F, Lemare M, Ahrens CH, Schreiber F, et al. Role of the flagellar
1145 hook in the structural development and antibiotic tolerance of Pseudomonas aeruginosa
1146 biofilms. The ISME Journal. 2022 Apr 1;16(4):1176–86.
1147 56. Dasgupta N, Wolfgang MC, Goodman AL, Arora SK, Jyot J, Lory S, et al. A four-tiered
1148 transcriptional regulatory circuit controls flagellar biogenesis in Pseudomonas aeruginosa.
1149 Molecular Microbiology. 2003;50(3):809–24.
1150 57. Francis VI, Stevenson EC, Porter SL. Two-component systems required for virulence in
1151 Pseudomonas aeruginosa. FEMS Microbiology Letters. 2017 Jun 15;364(11):fnx104.
1152 58. Kilmury SLN, Burrows LL. The Pseudomonas aeruginosa PilSR Two-Component System
1153 Regulates Both Twitching and Swimming Motilities. mBio. 2018 Jul
1154 24;9(4):10.1128/mbio.01310-18.
1155 59. Wiesmann CL, Zhang Y, Alford M, Hamilton CD, Dosanjh M, Thoms D, et al. The ColR/S two-
1156 component system is a conserved determinant of host association across Pseudomonas
1157 species. The ISME Journal. 2023 Feb 1;17(2):286–96.
1158 60. Gellatly SL, Bains M, Breidenstein EBM, Strehmel J, Reffuveille F, Taylor PK, et al. Novel roles for
1159 two-component regulatory systems in cytotoxicity and virulence-related properties in
1160 Pseudomonas aeruginosa. AIMS Microbiol. 2018 Mar 8;4(1):173–91.
1161 61. Latour X. The Evanescent GacS Signal. Microorganisms. 2020 Nov 6;8(11):1746.
1162 62. Davies JA, Harrison JJ, Marques LLR, Foglia GR, Stremick CA, Storey DG, et al. The GacS sensor
1163 kinase controls phenotypic reversion of small colony variants isolated from biofilms of
1164 Pseudomonas aeruginosa PA14. FEMS Microbiology Ecology. 2007;59(1):32–46.

1165 63. Weiler AJ, Spitz O, Gudzuhn M, Schott-Verdugo SN, Kamel M, Thiele B, et al. A phospholipase B
1166 from *Pseudomonas aeruginosa* with activity towards endogenous phospholipids affects biofilm
1167 assembly. Biochimica et Biophysica Acta (BBA) - Molecular and Cell Biology of Lipids. 2022 Apr
1168 1;1867(4):159101.
1169 64. Wu W, Huang J, Xu Z. Antibiotic influx and efflux in Pseudomonas aeruginosa: Regulation and
1170 therapeutic implications. Microbial Biotechnology. 2024;17(5):e14487.
1171 65. Alcalde-Rico M, Hernando-Amado S, Blanco P, Martínez JL. Multidrug Efflux Pumps at the
1172 Crossroad between Antibiotic Resistance and Bacterial Virulence. Front Microbiol [Internet].
1173 2016 Sep 21 [cited 2025 Jun 27];7. Available from:
1174 https://www.frontiersin.org/journals/microbiology/articles/10.3389/fmicb.2016.01483/full
1175 66. Jin Y, Yang H, Qiao M, Jin S. MexT Regulates the Type III Secretion System through MexS and
1176 PtrC in Pseudomonas aeruginosa. Journal of Bacteriology. 2011 Jan 3;193(2):399–410.
1177 67. Kristensen R, Andersen JB, Rybtke M, Jansen CU, Fritz BG, Kiilerich RO, et al. Inhibition of
1178 Pseudomonas aeruginosa quorum sensing by chemical induction of the MexEF-oprN efflux
1179 pump. Antimicrobial Agents and Chemotherapy. 2024 Jan 8;68(2):e01387-23.
1180 68. Bandyopadhyay S, Chandramouli K, Johnson MK. Iron–sulfur cluster biosynthesis. Biochemical
1181 Society Transactions. 2008 Nov 19;36(6):1112–9.
1182 69. De Los Santos PE, Parret AHA, De Mot R. Stress-related Pseudomonas genes involved in
1183 production of bacteriocin LlpA. FEMS Microbiology Letters. 2005 Mar 1;244(2):243–50.
1184 70. Michel L, González N, Jagdeep S, Nguyen-Ngoc T, Reimmann C. PchR-box recognition by the
1185 AraC-type regulator PchR of Pseudomonas aeruginosa requires the siderophore pyochelin as
1186 an effector. Molecular Microbiology. 2005;58(2):495–509.
1187 71. Trunk K, Benkert B, Quäck N, Münch R, Scheer M, Garbe J, et al. Anaerobic adaptation in
1188 Pseudomonas aeruginosa: definition of the Anr and Dnr regulons. Environmental Microbiology.
1189 2010;12(6):1719–33.
1190 72. Hausmann S, Gonzalez D, Geiser J, Valentini M. The DEAD-box RNA helicase RhlE2 is a global
1191 regulator of Pseudomonas aeruginosa lifestyle and pathogenesis. Nucleic Acids Research. 2021
1192 Jul 9;49(12):6925–40.
1193 73. Pu M, Sheng L, Song S, Gong T, Wood TK. Serine Hydroxymethyltransferase ShrA (PA2444)
1194 Controls Rugose Small-Colony Variant Formation in Pseudomonas aeruginosa. Front Microbiol
1195 [Internet]. 2018 Feb 27 [cited 2025 May 7];9. Available from:
1196 https://www.frontiersin.orghttps://www.frontiersin.org/journals/microbiology/articles/10.338
1197 9/fmicb.2018.00315/full
1198 74. Hung RJ, Chien HS, Lin RZ, Lin CT, Vatsyayan J, Peng HL, et al. Comparative analysis of two UDP-
1199 glucose dehydrogenases in Pseudomonas aeruginosa PAO1. J Biol Chem. 2007 Jun
1200 15;282(24):17738–48.
1201 75. Moskowitz SM, Ernst RK, Miller SI. PmrAB, a Two-Component Regulatory System of
1202 Pseudomonas aeruginosa That Modulates Resistance to Cationic Antimicrobial Peptides and
1203 Addition of Aminoarabinose to Lipid A. J Bacteriol. 2004 Jan;186(2):575–9.
1204 76. Salunkhe P, Smart CHM, Morgan JAW, Panagea S, Walshaw MJ, Hart CA, et al. A Cystic Fibrosis
1205 Epidemic Strain of Pseudomonas aeruginosa Displays Enhanced Virulence and Antimicrobial
1206 Resistance. Journal of Bacteriology. 2005 Jul;187(14):4908–20.
1207 77. Bugg TD, Walsh CT. Intracellular steps of bacterial cell wall peptidoglycan biosynthesis:
1208 enzymology, antibiotics, and antibiotic resistance. Nat Prod Rep. 1992 Jun;9(3):199–215.
1209 78. El Zoeiby A, Sanschagrin F, Lamoureux J, Darveau A, Levesque RC. Cloning, over-expression and
1210 purification of Pseudomonas aeruginosa murC encoding uridine diphosphate N-
1211 acetylmuramate: l-alanine ligase. FEMS Microbiology Letters. 2000 Feb 1;183(2):281–8.

1212 79. Tang J, Luo M, Niu S, Zhou H, Cai X, Zhang W, et al. The Crystal Structure of Hexamer RraA from
1213 Pseudomonas Aeruginosa Reveals Six Conserved Protein–Protein Interaction Sites. Protein J.
1214 2010 Nov 1;29(8):583–90.
1215 80. Lossi NS, Manoli E, Simpson P, Jones C, Hui K, Dajani R, et al. The archetype Pseudomonas
1216 aeruginosa proteins TssB and TagJ form a novel subcomplex in the bacterial type VI secretion
1217 system. Molecular Microbiology. 2012;86(2):437–56.
1218 81. Chevalier S, Bouffartigues E, Bodilis J, Maillot O, Lesouhaitier O, Feuilloley MGJ, et al. Structure,
1219 function and regulation of Pseudomonas aeruginosa porins. FEMS Microbiology Reviews. 2017
1220 Sep 1;41(5):698–722.
1221 82. Nguyen KV, Nguyen ,Trung Vu, Nguyen ,Hang Thi Thuy, and Le DV. Mutations in the gyrA, parC,
1222 and mexR genes provide functional insights into the fluoroquinolone-resistant Pseudomonas
1223 aeruginosa isolated in Vietnam. Infection and Drug Resistance. 2018 Feb 2;11:275–82.
1224 83. Arabameri N, Heshmatipour Z, Eftekhar Ardebili S, Jafari Bidhendi Z. The role of Gene
1225 Mutations (gyrA, parC) in Resistance to Ciprofloxacin in Clinical Isolates of Pseudomonas
1226 Aeruginosa. Iran J Pathol. 2021;16(4):426–32.
1227 84. Ortiz-Severín J, Varas M, Bravo-Toncio C, Guiliani N, Chávez FP. Multiple antibiotic susceptibility
1228 of polyphosphate kinase mutants (ppk1 and ppk2) from Pseudomonas aeruginosa PAO1 as
1229 revealed by global phenotypic analysis. biol res. 2015 Apr 25;48(1):22.
1230 85. Huang Q, Yang J, Li C, Song Y, Zhu Y, Zhao N, et al. Structural characterization of PaFkbA: A
1231 periplasmic chaperone from *Pseudomonas aeruginosa*. Computational and Structural
1232 Biotechnology Journal. 2021 Jan 1;19:2460–7.
1233 86. Alam A, Bröms JE, Kumar R, Sjöstedt A. The Role of ClpB in Bacterial Stress Responses and
1234 Virulence. Front Mol Biosci [Internet]. 2021 Apr 22 [cited 2025 Jun 29];8. Available from:
1235 https://www.frontiersin.org/journals/molecular-
1236 biosciences/articles/10.3389/fmolb.2021.668910/full
1237 87. Nolan LM, Cain AK, Clamens T, Furniss RCD, Manoli E, Sainz-Polo MA, et al. Identification of
1238 Tse8 as a Type VI secretion system toxin from Pseudomonas aeruginosa that targets the
1239 bacterial transamidosome to inhibit protein synthesis in prey cells. Nat Microbiol. 2021
1240 Sep;6(9):1199–210.
1241 88. Nikel PI, Pérez-Pantoja D, de Lorenzo V. Pyridine nucleotide transhydrogenases enable redox
1242 balance of Pseudomonas putida during biodegradation of aromatic compounds. Environ
1243 Microbiol. 2016 Oct;18(10):3565–82.
1244 89. Li C, Wally H, Miller SJ, Lu CD. The Multifaceted Proteins MvaT and MvaU, Members of the H-
1245 NS Family, Control Arginine Metabolism, Pyocyanin Synthesis, and Prophage Activation in
1246 Pseudomonas aeruginosa PAO1. Journal of Bacteriology. 2009 Oct 15;191(20):6211–8.
1247 90. Williams McMackin EA, Marsden AE, Yahr TL. H-NS Family Members MvaT and MvaU Regulate
1248 the Pseudomonas aeruginosa Type III Secretion System. Journal of Bacteriology. 2019 Jun
1249 21;201(14):10.1128/jb.00054-19.
1250 91. Castang S, Dove SL. Basis for the Essentiality of H-NS Family Members in Pseudomonas
1251 aeruginosa. Journal of Bacteriology. 2012 Aug 28;194(18):5101–9.
1252 92. Nganje CN, Haynes SA, Qabar CM, Lent RC, Ghanem ENB, Shainheit MG. PepN is a non-
1253 essential, cell wall-localized protein that contributes to neutrophil elastase-mediated killing of
1254 Streptococcus pneumoniae. PLOS ONE. 2019 Feb 1;14(2):e0211632.
1255 93. Lequette Y, Rollet E, Delangle A, Greenberg EP, Bohin JP. Linear osmoregulated periplasmic
1256 glucans are encoded by the opgGH locus of Pseudomonas aeruginosa. Microbiology.
1257 2007;153(10):3255–63.

1258 94. Hauser AR, Kang PJ, Engel JN. PepA, a secreted protein of Pseudomonas aeruginosa, is
1259 necessary for cytotoxicity and virulence. Mol Microbiol. 1998 Feb;27(4):807–18.
1260 95. Tipton KA, Coleman JP, Pesci EC. Post-transcriptional regulation of gene PA5507 controls
1261 Pseudomonas quinolone signal concentration in P. aeruginosa. Molecular Microbiology.
1262 2015;96(3):670–83.
1263 96. Lin Q, Wang H, Huang J, Liu Z, Chen Q, Yu G, et al. Spermidine Is an Intercellular Signal
1264 Modulating T3SS Expression in Pseudomonas aeruginosa. Microbiology Spectrum. 2022 Apr
1265 18;10(3):e00644-22.
1266 97. Wu D, Lim SC, Dong Y, Wu J, Tao F, Zhou L, et al. Structural Basis of Substrate Binding Specificity
1267 Revealed by the Crystal Structures of Polyamine Receptors SpuD and SpuE from *Pseudomonas*
1268 *aeruginosa*. Journal of Molecular Biology. 2012 Mar 9;416(5):697–712.
1269 98. Marquart ME, Caballero AR, Chomnawang M, Thibodeaux BA, Twining SS, O'Callaghan RJ.
1270 Identification of a Novel Secreted Protease from Pseudomonas aeruginosa that Causes Corneal
1271 Erosions. Investigative Ophthalmology & Visual Science. 2005 Oct 1;46(10):3761–8.
1272 99. Lee C, Kim MI, Park J, Kim J, Oh H, Cho Y, et al. Crystal structure of the *Pseudomonas*
1273 *aeruginosa* PA0423 protein and its functional implication in antibiotic sequestration.
1274 Biochemical and Biophysical Research Communications. 2020 Jul 12;528(1):85–91.
1275 100. Romsang A, Duang-nkern J, Saninjuk K, Vattanaviboon P, Mongkolsuk S. Pseudomonas
1276 aeruginosa nfuA: Gene regulation and its physiological roles in sustaining growth under stress
1277 and anaerobic conditions and maintaining bacterial virulence. PLOS ONE. 2018 Aug
1278 9;13(8):e0202151.
1279 101. Daung-nkern J, Vattanaviboon P, Mongkolsuk S. Inactivation of nfuA enhances susceptibility of
1280 Pseudomonas aeruginosa to fluoroquinolone antibiotics. Journal of Antimicrobial
1281 Chemotherapy. 2010 Aug 1;65(8):1831–2.
1282 102. Drabinska J, Ziecina M, Modzelan M, Jagura-Burdzy G, Kraszewska E. Individual Nudix
1283 hydrolases affect diverse features of Pseudomonas aeruginosa. Microbiologyopen. 2020 May
1284 17;9(8):e1052.
1285 103. Semmler ABT, Whitchurch CB, Leech AJ, Mattick JS. Identification of a novel gene, fimV,
1286 involved in twitching motility in Pseudomonas aeruginosaThe GenBank accession number for
1287 the sequence determined in this work is U93274. Microbiology. 2000;146(6):1321–32.
1288 104. Michel GPF, Aguzzi A, Ball G, Soscia C, Bleves S, Voulhoux R. Role of fimV in type II secretion
1289 system-dependent protein secretion of Pseudomonas aeruginosa on solid medium.
1290 Microbiology. 2011;157(7):1945–54.
1291 105. Shen L, Gao L, Yang M, Zhang J, Wang Y, Feng Y, et al. Deletion of the PA4427-PA4431 Operon
1292 of Pseudomonas aeruginosa PAO1 Increased Antibiotics Resistance and Reduced Virulence and
1293 Pathogenicity by Affecting Quorum Sensing and Iron Uptake. Microorganisms. 2021 May
1294 14;9(5):1065.
1295 106. Duque E, de la Torre J, Bernal P, Molina-Henares MA, Alaminos M, Espinosa-Urgel M, et al.
1296 Identification of reciprocal adhesion genes in pathogenic and non-pathogenic Pseudomonas.
1297 Environmental Microbiology. 2013;15(1):36–48.
1298 107. Yoon SS, Hennigan RF, Hilliard GM, Ochsner UA, Parvatiyar K, Kamani MC, et al. Pseudomonas
1299 aeruginosa Anaerobic Respiration in Biofilms: Relationships to Cystic Fibrosis Pathogenesis.
1300 Developmental Cell. 2002;
1301 108. König J, Schreiber R, Voelcker T, Mall M, Kunzelmann K. The cystic fibrosis transmembrane
1302 conductance regulator (CFTR) inhibits ENaC through an increase in the intracellular Cl–
1303 concentration. EMBO Rep. 2001 Nov 15;2(11):1047–51.

1304 109. Cowley ES, Kopf SH, LaRiviere A, Ziebis W, Newman DK. Pediatric Cystic Fibrosis Sputum Can Be
1305 Chemically Dynamic, Anoxic, and Extremely Reduced Due to Hydrogen Sulfide Formation.
1306 mBio. 2015 Jul 28;6(4):10.1128/mbio.00767-15.
1307 110. Line L, Alhede M, Kolpen M, Kühl M, Ciofu O, Bjarnsholt T, et al. Physiological levels of nitrate
1308 support anoxic growth by denitrification of Pseudomonas aeruginosa at growth rates reported
1309 in cystic fibrosis lungs and sputum. Front Microbiol. 2014 Oct 24;5:554.
1310 111. Borriello G, Richards L, Ehrlich GD, Stewart PS. Arginine or Nitrate Enhances Antibiotic
1311 Susceptibility of Pseudomonas aeruginosa in Biofilms. Antimicrobial Agents and
1312 Chemotherapy. 2006 Jan;50(1):382–4.
1313 112. Carey CJ, Duggan N, Drabinska J, McClean S. Harnessing hypoxia: bacterial adaptation and
1314 chronic infection in cystic fibrosis. FEMS Microbiology Reviews. 2025 Jan 1;49:fuaf018.
1315 113. Tribelli PM, Lujan AM, Pardo A, Ibarra JG, Fernández Do Porto D, Smania A, et al. Core regulon
1316 of the global anaerobic regulator Anr targets central metabolism functions in Pseudomonas
1317 species. Sci Rep. 2019 Jun 21;9(1):9065.
1318 114. Papa R, Imperlini E, Trecca M, Paris I, Vrenna G, Artini M, et al. Virulence of Pseudomonas
1319 aeruginosa in Cystic Fibrosis: Relationships between Normoxia and Anoxia Lifestyle.
1320 Antibiotics. 2024 Jan;13(1):1.
1321 115. Kamath KS, Krisp C, Chick J, Pascovici D, Gygi SP, Molloy MP. Pseudomonas aeruginosa
1322 Proteome under Hypoxic Stress Conditions Mimicking the Cystic Fibrosis Lung. J Proteome Res.
1323 2017 Oct 6;16(10):3917–28.
1324 116. Ashish A, Paterson S, Mowat E, Fothergill JL, Walshaw MJ, Winstanley C. Extensive
1325 diversification is a common feature of Pseudomonas aeruginosa populations during respiratory
1326 infections in cystic fibrosis. J Cyst Fibros. 2013 Dec;12(6):790–3.
1327 117. Flynn KM, Dowell G, Johnson TM, Koestler BJ, Waters CM, Cooper VS. Evolution of Ecological
1328 Diversity in Biofilms of Pseudomonas aeruginosa by Altered Cyclic Diguanylate Signaling.
1329 Journal of Bacteriology. 2016 Sep 9;198(19):2608–18.
1330 118. Jorth P, Staudinger BJ, Wu X, Hisert K, Hayden H, Garudathri J, et al. Regional Isolation Drives
1331 Bacterial Diversification within Cystic Fibrosis Lungs. Cell Host Microbe. 2015 Sep 9;18(3):307–
1332 19.
1333 119. Markussen T, Marvig RL, Gómez-Lozano M, Aanæs K, Burleigh AE, Høiby N, et al.
1334 Environmental heterogeneity drives within-host diversification and evolution of Pseudomonas
1335 aeruginosa. mBio. 2014 Sep 16;5(5):e01592-01514.
1336 120. Winstanley C, O'Brien S, Brockhurst MA. Pseudomonas aeruginosa Evolutionary Adaptation
1337 and Diversification in Cystic Fibrosis Chronic Lung Infections. Trends Microbiol. 2016
1338 May;24(5):327–37.
1339 121. Letunic I, Bork P. Interactive Tree of Life (iTOL) v6: recent updates to the phylogenetic tree
1340 display and annotation tool. Nucleic Acids Research. 2024 Jul 5;52(W1):W78–82.
1341 122. Bueno E, Mesa S, Bedmar EJ, Richardson DJ, Delgado MJ. Bacterial Adaptation of Respiration
1342 from Oxic to Microoxic and Anoxic Conditions: Redox Control. Antioxidants & Redox Signaling.
1343 2012 Apr 15;16(8):819–52.
1344 123. Scribani Rossi C, Eckartt K, Scarchilli E, Angeli S, Price-Whelan A, Di Matteo A, et al. Molecular
1345 insights into RmcA-mediated c-di-GMP consumption: Linking redox potential to biofilm
1346 morphogenesis in Pseudomonas aeruginosa. Microbiol Res. 2023 Dec;277:127498.
1347 124. Schmidt A, Hammerbacher AS, Bastian M, Nieken KJ, Klockgether J, Merighi M, et al. Oxygen-
1348 dependent regulation of c-di-GMP synthesis by SadC controls alginate production in
1349 seudomonas aeruginosa. Environmental Microbiology. 2016;18(10):3390–402.

125. An S, Wu J, Zhang LH. Modulation of Pseudomonas aeruginosa Biofilm Dispersal by a Cyclic-Di-GMP Phosphodiesterase with a Putative Hypoxia-Sensing Domain. Appl Environ Microbiol. 2010 Dec;76(24):8160–73.
126. Wang H, de Carvalho LPS. Metabolomic profiling reveals bacterial metabolic adaptation strategies and new metabolites. Current Opinion in Chemical Biology. 2023 Jun 1;74:102287.
127. Banerjee P, Sahoo PK, Sheenu null, Adhikary A, Ruhal R, Jain D. Molecular and structural facets of c-di-GMP signalling associated with biofilm formation in Pseudomonas aeruginosa. Mol Aspects Med. 2021 Oct;81:101001.
128. Gupta K, Liao J, Petrova OE, Cherny KE, Sauer K. Elevated levels of the second messenger c-di-GMP contribute to antimicrobial resistance of Pseudomonas aeruginosa. Mol Microbiol. 2014 May;92(3):488–506.
129. Arai H. Regulation and Function of Versatile Aerobic and Anaerobic Respiratory Metabolism in Pseudomonas aeruginosa. Front Microbiol [Internet]. 2011 May 5 [cited 2025 May 20];2. Available from: https://www.frontiersin.org/journals/microbiology/articles/10.3389/fmicb.2011.00103/full
130. O'Connor JR, Kuwada NJ, Huangyutitham V, Wiggins PA, Harwood CS. Surface sensing and lateral subcellular localization of WspA, the receptor in a chemosensory-like system leading to c-di-GMP production. Mol Microbiol. 2012 Nov;86(3):720–9.
131. Dev IK, Harvey RJ. Regulation of synthesis of serine hydroxymethyltransferase in chemostat cultures of Escherichia coli. Journal of Biological Chemistry. 1984 Jul 10;259(13):8394–401.
132. Attila C, Ueda A, Wood TK. PA2663 (PpyR) increases biofilm formation in Pseudomonas aeruginosa PAO1 through the psl operon and stimulates virulence and quorum-sensing phenotypes. Appl Microbiol Biotechnol. 2008 Feb;78(2):293–307.
133. Brencic A, McFarland KA, McManus HR, Castang S, Mogno I, Dove SL, et al. The GacS/GacA signal transduction system of Pseudomonas aeruginosa acts exclusively through its control over the transcription of the RsmY and RsmZ regulatory small RNAs. Molecular Microbiology. 2009;73(3):434–45.
134. Yan J, Deforet M, Boyle KE, Rahman R, Liang R, Okegbe C, et al. Bow-tie signaling in c-di-GMP: Machine learning in a simple biochemical network. PLOS Computational Biology. 2017 Aug 2;13(8):e1005677.
135. Besse A, Groleau MC, Trottier M, Vincent AT, Déziel E. Pseudomonas aeruginosa Strains from Both Clinical and Environmental Origins Readily Adopt a Stable Small-Colony-Variant Phenotype Resulting from Single Mutations in c-di-GMP Pathways. J Bacteriol. 2022 Oct 18;204(10):e0018522.
136. Besse A, Groleau MC, Déziel E. Emergence of Small Colony Variants Is an Adaptive Strategy Used by Pseudomonas aeruginosa to Mitigate the Effects of Redox Imbalance. mSphere. 2023 Feb 28;8(2):e00057-23.
137. Johns BE, Purdy KJ, Tucker NP, Maddocks SE. Phenotypic and Genotypic Characteristics of Small Colony Variants and Their Role in Chronic Infection. Microbiol Insights. 2015 Jan 1;8:MBI.S25800.
138. Ryan H, Ballard E, Stockwell RE, Duplancic C, Thomson RM, Smith K, et al. A systematic review of the clinical impact of small colony variants in patients with cystic fibrosis. BMC Pulm Med. 2023 Sep 1;23(1):323.
139. Schneider M, Mühlemann K, Droz S, Couzinet S, Casaulta C, Zimmerli S. Clinical Characteristics Associated with Isolation of Small-Colony Variants of Staphylococcus aureus and Pseudomonas aeruginosa from Respiratory Secretions of Patients with Cystic Fibrosis. Journal of Clinical Microbiology. 2008 Mar 5;46(5):1832.

140. Malone JG. Role of small colony variants in persistence of Pseudomonas aeruginosa infections in cystic fibrosis lungs. Infection and Drug Resistance. 2015 Jul 29;8(null):237–47.
141. Hoffman LR, Déziel E, D'Argenio DA, Lépine F, Emerson J, McNamara S, et al. Selection for Staphylococcus aureus small-colony variants due to growth in the presence of Pseudomonas aeruginosa. Proceedings of the National Academy of Sciences. 2006 Dec 26;103(52):19890–5.
142. Bjarnsholt T, Jensen PØ, Fiandaca MJ, Pedersen J, Hansen CR, Andersen CB, et al. Pseudomonas aeruginosa biofilms in the respiratory tract of cystic fibrosis patients. Pediatr Pulmonol. 2009 Jun;44(6):547–58.
143. Høiby N, Ciofu O, Bjarnsholt T. Pseudomonas Aeruginosa Biofilms in Cystic fibrosis. Future Microbiology. 2010 Nov 1;5(11):1663–74.
144. Maurice NM, Bedi B, Sadikot RT. Pseudomonas aeruginosa Biofilms: Host Response and Clinical Implications in Lung Infections. Am J Respir Cell Mol Biol. 2018 Apr;58(4):428–39.
145. Klementiev AD, Jin Z, Whiteley M. Micron Scale Spatial Measurement of the O2 Gradient Surrounding a Bacterial Biofilm in Real Time. mBio. 2020 Oct 20;11(5):10.1128/mbio.02536-20.
146. Wu Y, Klapper I, Stewart PS. Hypoxia arising from concerted oxygen consumption by neutrophils and microorganisms in biofilms. Pathogens and Disease. 2018 Apr 23;76(4):fty043.
147. Bowler P, Murphy C, Wolcott R. Biofilm exacerbates antibiotic resistance: Is this a current oversight in antimicrobial stewardship? Antimicrob Resist Infect Control. 2020 Oct 20;9(1):162.
148. Liang Z, Nilsson M, Kragh KN, Hedal I, Alcàcer-Almansa J, Kiilerich RO, et al. The role of individual exopolysaccharides in antibiotic tolerance of Pseudomonas aeruginosa aggregates. Front Microbiol. 2023 Jul 2;14(1187708).
149. Oladosu VI, Park S, Sauer K. Flip the switch: the role of FleQ in modulating the transition between the free-living and sessile mode of growth in Pseudomonas aeruginosa. Journal of Bacteriology. 2024 Mar 4;206(3):e00365-23.
150. Sindeldecker D, Stoodley P. The many antibiotic resistance and tolerance strategies of *Pseudomonas aeruginosa*. Biofilm. 2021 Dec 1;3:100056.
151. Borriello G, Werner E, Roe F, Kim AM, Ehrlich GD, Stewart PS. Oxygen Limitation Contributes to Antibiotic Tolerance of Pseudomonas aeruginosa in Biofilms. Antimicrobial Agents and Chemotherapy. 2004 Jul;48(7):2659–64.
152. Schaible B, Taylor CT, Schaffer K. Hypoxia Increases Antibiotic Resistance in Pseudomonas aeruginosa through Altering the Composition of Multidrug Efflux Pumps. Antimicrobial Agents and Chemotherapy. 2012 Mar 16;56(4):2114–8.
153. Zhao X, Drlica K. Reactive oxygen species and the bacterial response to lethal stress. Current opinion in microbiology. 2014 Jul 30;0:1.
154. Macfarlane ELA, Kwasnicka A, Ochs MM, Hancock REW. PhoP–PhoQ homologues in Pseudomonas aeruginosa regulate expression of the outer-membrane protein OprH and polymyxin B resistance. Molecular Microbiology. 1999;34(2):305–16.
155. Edrington TC, Kintz E, Goldberg JB, Tamm LK. Structural Basis for the Interaction of Lipopolysaccharide with Outer Membrane Protein H (OprH) from Pseudomonas aeruginosa*. Journal of Biological Chemistry. 2011 Nov 11;286(45):39211–23.
156. Hameed P S, Manjrekar P, Chinnapattu M, Humnabadkar V, Shanbhag G, Kedari C, et al. Pyrazolopyrimidines Establish MurC as a Vulnerable Target in Pseudomonas aeruginosa and Escherichia coli. ACS Chem Biol. 2014 Oct 17;9(10):2274–82.
157. Nalca Y, Jänsch L, Bredenbruch F, Geffers R, Buer J, Häussler S. Quorum-Sensing Antagonistic Activities of Azithromycin in Pseudomonas aeruginosa PAO1: a Global Approach. Antimicrob Agents Chemother. 2006 May;50(5):1680–8.

1443 158. Rausch M, Deisinger JP, Ulm H, Müller A, Li W, Hardt P, et al. Coordination of capsule assembly
1444 and cell wall biosynthesis in Staphylococcus aureus. Nat Commun. 2019 Mar 29;10(1):1404.
1445 159. Higgins PG, Fluit AC, Milatovic D, Verhoef J, Schmitz FJ. Mutations in GyrA, ParC, MexR and
1446 NfxB in clinical isolates of *Pseudomonas aeruginosa*. International Journal of Antimicrobial
1447 Agents. 2003 May 1;21(5):409–13.
1448 160. Hunter RC, Asfour F, Dingemans J, Osuna BL, Samad T, Malfroot A, et al. Ferrous Iron Is a
1449 Significant Component of Bioavailable Iron in Cystic Fibrosis Airways. mBio. 2013 Aug
1450 20;4(4):10.1128/mbio.00557-13.
1451 161. Moreau-Marquis S, Bomberger JM, Anderson GG, Swiatecka-Urban A, Ye S, O'Toole GA, et al.
1452 The DeltaF508-CFTR mutation results in increased biofilm formation by Pseudomonas
1453 aeruginosa by increasing iron availability. Am J Physiol Lung Cell Mol Physiol. 2008
1454 Jul;295(1):L25-37.
1455 162. Schalk IJ, Perraud Q. and its multiple strategies to access iron. Environmental Microbiology.
1456 2023;25(4):811–31.
1457 163. Reid DW, Carroll V, O'May C, Champion A, Kirov SM. Increased airway iron as a potential factor
1458 in the persistence of Pseudomonas aeruginosa infection in cystic fibrosis. European Respiratory
1459 Journal. 2007 Aug 1;30(2):286–92.
1460 164. Frangipani E, Visaggio D, Heeb S, Kaever V, Cámara M, Visca P, et al. The Gac/Rsm and cyclic-di-
1461 GMP signalling networks coordinately regulate iron uptake in seudomonas aeruginosa.
1462 Environmental Microbiology. 2014;16(3):676–88.
1463 165. Banin E, Brady KM, Greenberg EP. Chelator-induced dispersal and killing of Pseudomonas
1464 aeruginosa cells in a biofilm. Appl Environ Microbiol. 2006 Mar;72(3):2064–9.
1465 166. Miller HK, Auerbuch V. Bacterial iron-sulfur cluster sensors in mammalian pathogens.
1466 Metallomics. 2015 Jun 10;7(6):943–56.
1467 167. Konings AF, Martin LW, Sharples KJ, Roddam LF, Latham R, Reid DW, et al. Pseudomonas
1468 aeruginosa Uses Multiple Pathways To Acquire Iron during Chronic Infection in Cystic Fibrosis
1469 Lungs. Infection and Immunity. 2013 Jul 11;81(8):2697–704.
1470 168. Schaible B, Rodriguez J, Garcia A, von Kriegsheim A, McClean S, Hickey C, et al. Hypoxia
1471 Reduces the Pathogenicity of Pseudomonas aeruginosa by Decreasing the Expression of
1472 Multiple Virulence Factors. J Infect Dis. 2017 May 1;215(9):1459–67.
1473 169. Weimann A, Dinan AM, Ruis C, Bernut A, Pont S, Brown K, et al. Evolution and host-specific
1474 adaptation of Pseudomonas aeruginosa. Science. 2024 Jul 5;385(6704):eadi0908.
1475 170. Amoureux L, Bador J, Fardeheb S, Mabille C, Couchot C, Massip C, et al. Detection of
1476 Achromobacter xylosoxidans in Hospital, Domestic, and Outdoor Environmental Samples and
1477 Comparison with Human Clinical Isolates. Appl Environ Microbiol. 2013 Dec;79(23):7142–9.
1478 171. Crone S, Vives-Flórez M, Kvich L, Saunders AM, Malone M, Nicolaisen MH, et al. The
1479 environmental occurrence of Pseudomonas aeruginosa. APMIS. 2020;128(3):220–31.
1480 172. Honda JR, Virdi R, Chan ED. Global Environmental Nontuberculous Mycobacteria and Their
1481 Contemporaneous Man-Made and Natural Niches. Front Microbiol. 2018 Aug 30;9.
1482 173. Honda JR, Virdi R, Chan ED. Global Environmental Nontuberculous Mycobacteria and Their
1483 Contemporaneous Man-Made and Natural Niches. Front Microbiol. 2018;9:2029.
1484 174. Price CTD, Hanford HE, Al-Quadan T, Santic M, Shin CJ, Da'as MSJ, et al. Amoebae as training
1485 grounds for microbial pathogens. mBio. 2024 Jul 8;15(8):e00827-24.
1486 175. Mullard A. 2023 FDA approvals. Nat Rev Drug Discov. 2024 Feb;23(2):88–95.

176. Rashid MH, Kornberg A. Inorganic polyphosphate is needed for swimming, swarming, and twitching motilities of Pseudomonas aeruginosa. Proc Natl Acad Sci U S A. 2000 Apr 25;97(9):4885–90.
177. Arora NK, Verma M. Modified microplate method for rapid and efficient estimation of siderophore produced by bacteria. 3 Biotech. 2017 Dec;7(6):381.
178. Roy AB, Petrova OE, Sauer K. Extraction and Quantification of Cyclic Di-GMP from P. aeruginosa. Bio Protoc. 2013;3(14):e828.

Supporting information captions

S1. Figure. Differences in growth patterns of the *P. aeruginosa* AMT 0023-30 early infection strain with different inoculation volumes.

S2. Figure. Differences in doubling times of the *P. aeruginosa* AMT 002330 early infection strain in hypoxic and normoxic conditions. A. OD_{600} measurements over time. **B.** CFU/ml counts over time **C.** OD_{600} to CFU/ml trend lines and linear regression calculations. **D.** Differences in generation times in normoxia and hypoxia.

S3. Figure. Stability of SCVs in normoxic conditions. A. Photograph of different *P. aeruginosa* colony variants streaked on LB agar and grown overnight in normoxic conditions. **B.** Enlarged fragment of photograph in section A.

S4. Table. Proteomic analysis of long-term hypoxia-adapted *P. aeruginosa* isolates. A. All proteins differentially expressed between HACs and the ancestral strain (D0), NACs and the ancestral strain (D0) or HACs and NACs. **B.** Proteins not detected in at least two replicates in at least one of the groups (Day 0, HACs, NACs). C. All proteins detected in the proteomics analysis of the ancestral strain, HACs and NACs

S5. Table. Functional enrichment of the 89 proteins of interest significantly altered in abundance after long-term adaptation of *P. aeruginosa* to hypoxia

S6. Figure. Effects of long-term hypoxia adaptation on intracellular c-di-GMP concentrations. The graph represents the concentration of c-di-GMP in the cell extract from an equivalent of 4 ml of culture of OD_{600} = 1.8. No statistically significant differences between cultures were shown with the Brown-Forsythe ANOVA test. E: early infection clinical strain (AMT 0023-30); L: late infection clinical strain (AMT 0023-34); N1, N2, N3: 28-day normoxia-adapted populations; H1, H2, H3: 28-day hypoxia adapted populations.

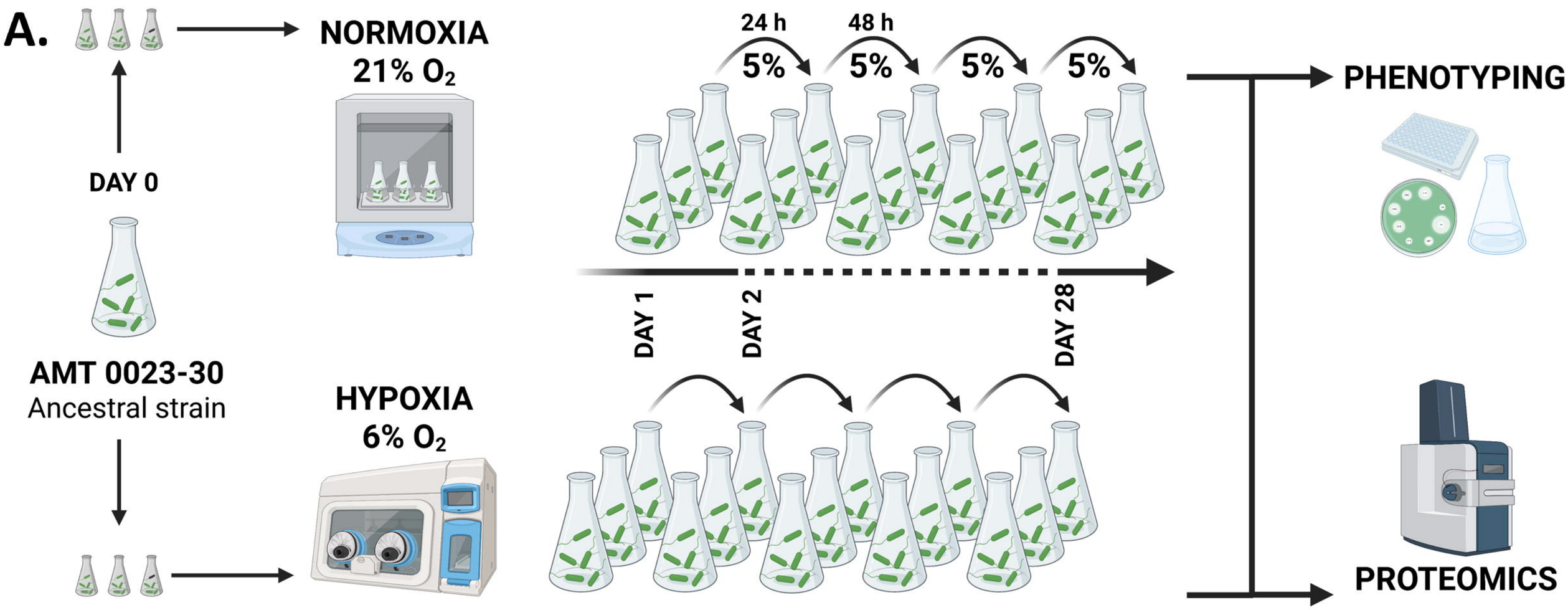
A.
NORMOXIA
21% O2
DAY 0
AMT 0023-30
Ancestral strain
HYPOXIA
6% O2
24 h
48 h
5%
5%
5%
5%
DAY 1
DAY 2
DAY 28
PHENOTYPING
PROTEOMICS

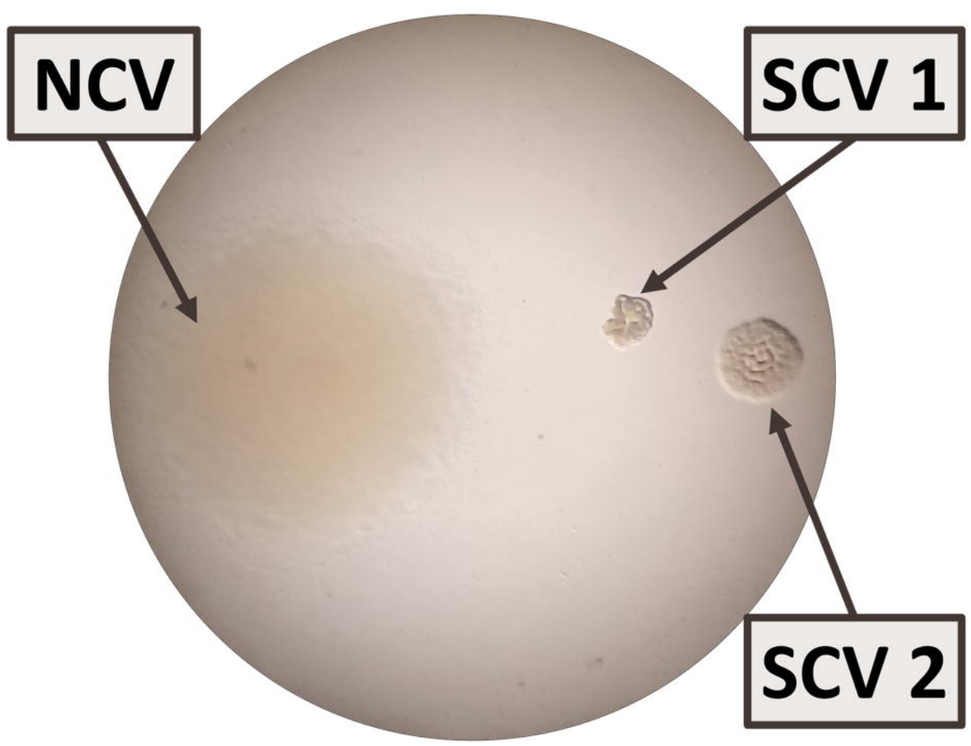
B.
NCV
SCV 1
SCV 2

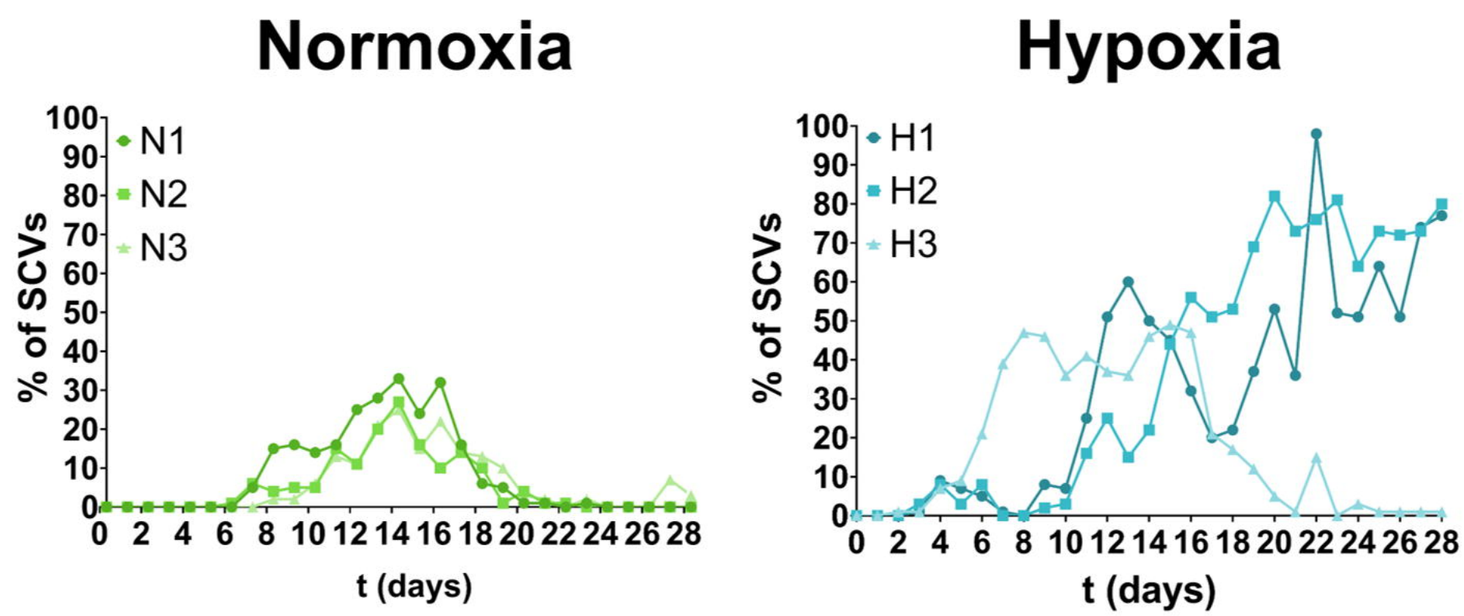
C.
Normoxia
Hypoxia
N1
N2
N3
H1
H2
H3
% of SCVs
t (days)

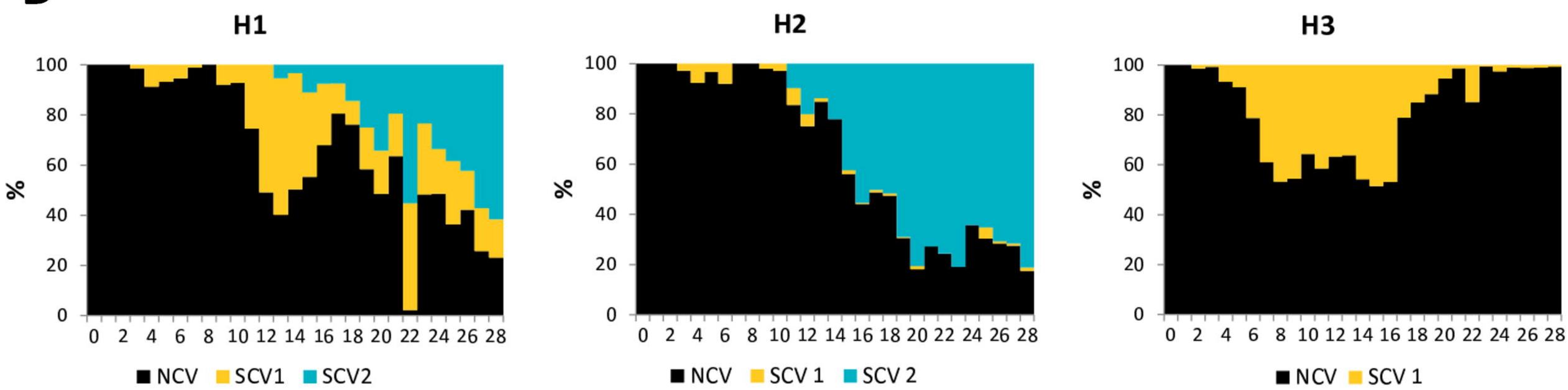
D
H1
H2
H3
%
NCV
SCV1
SCV2
SCV 1
SCV 2

A.

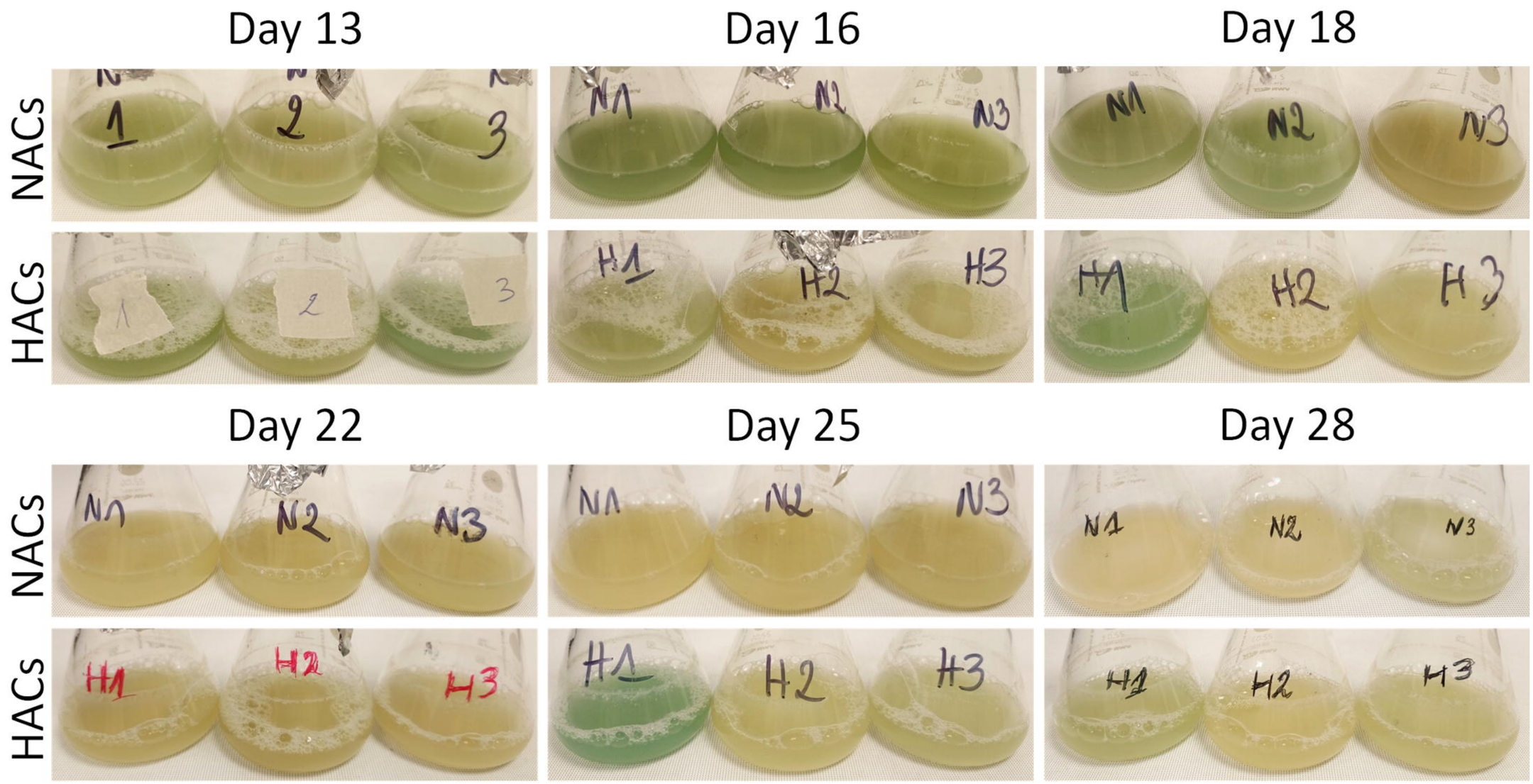
Day 13
Day 16
Day 18
Day 22
Day 25
Day 28
NACs
HACs

B.

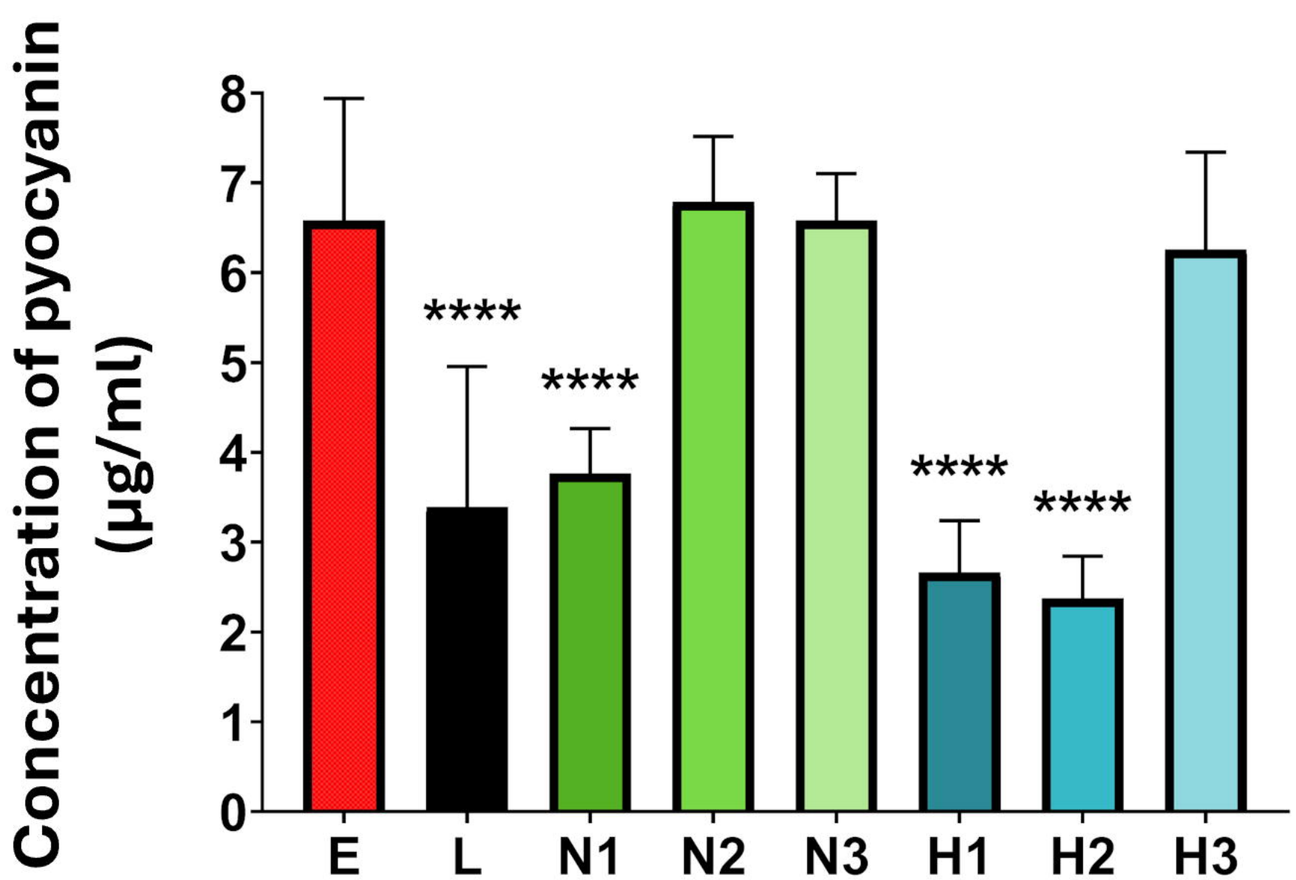
Concentration of pyocyanin (µg/ml)
0
1
2
3
4
5
6
7
8
****
****
****
****
E
L
N1
N2
N3
H1
H2
H3

C.

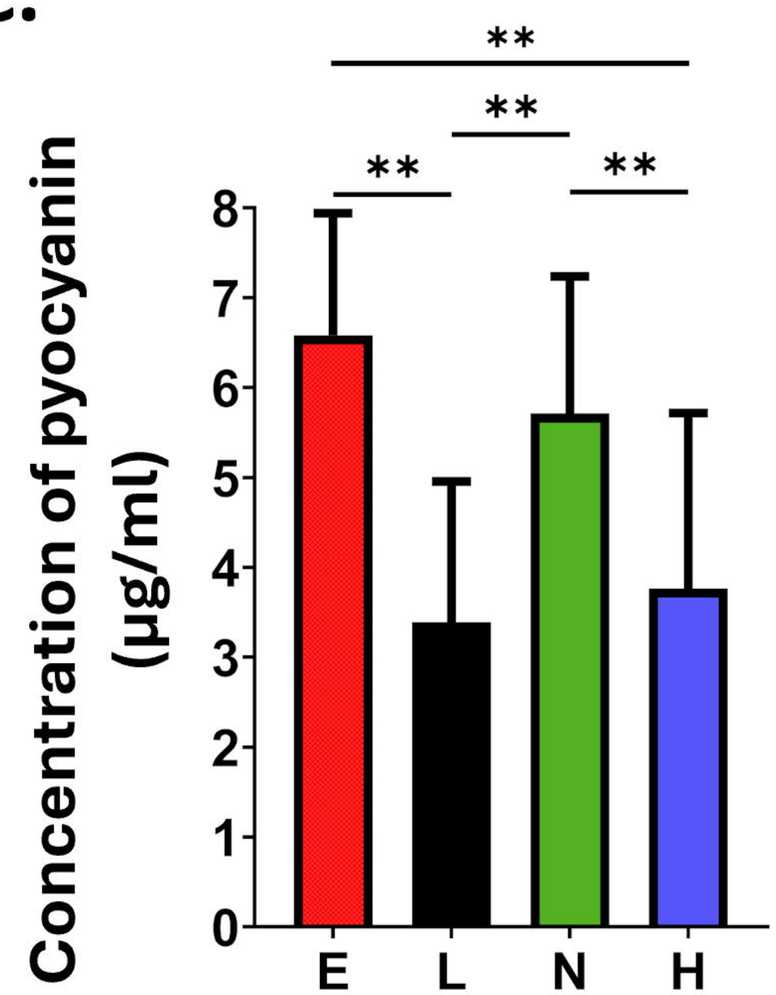
Concentration of pyocyanin (µg/ml)
0
1
2
3
4
5
6
7
8
**
**
**
**
E
L
N
H

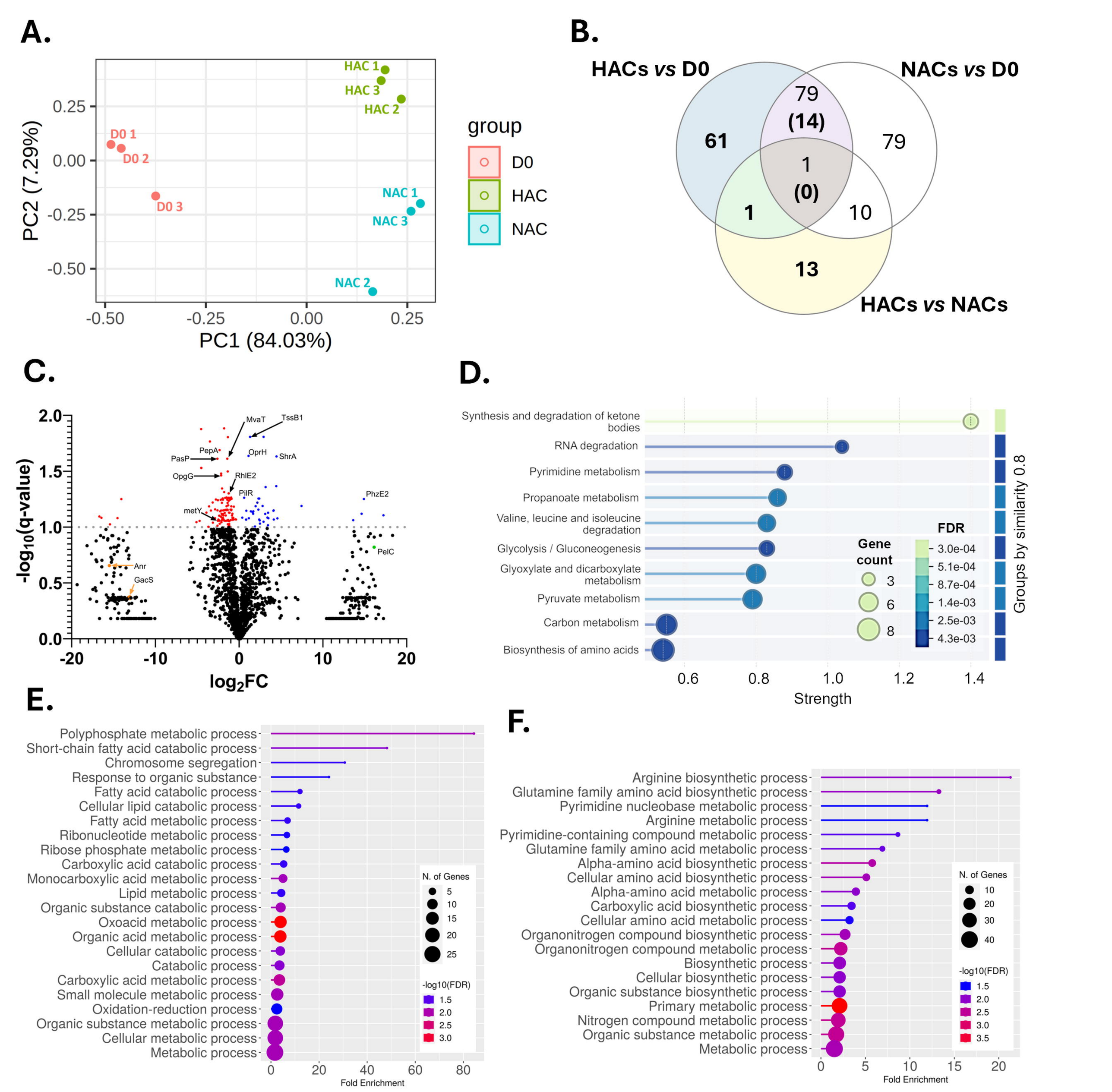
A.
HAC 1
HAC 3
HAC 2
D0 1
D0 2
D0 3
NAC 1
NAC 3
NAC 2
PC2 (7.29%)
PC1 (84.03%)
group
D0
HAC
NAC
B.
HACs vs D0
NACs vs D0
HACs vs NACs
61
79
(14)
79
1
(0)
1
10
13
C.
-log10(q-value)
log2FC
MvaT
TssB1
PepA
PasP
OprH
ShrA
OpgG
RhlE2
PilR
PhzE2
metY
PelC
Anr
GacS
D.
Synthesis and degradation of ketone bodies
RNA degradation
Pyrimidine metabolism
Propanoate metabolism
Valine, leucine and isoleucine degradation
Glycolysis / Gluconeogenesis
Glyoxylate and dicarboxylate metabolism
Pyruvate metabolism
Carbon metabolism
Biosynthesis of amino acids
Strength
Groups by similarity 0.8
Gene count
FDR
E.
Polyphosphate metabolic process
Short-chain fatty acid catabolic process
Chromosome segregation
Response to organic substance
Fatty acid catabolic process
Cellular lipid catabolic process
Fatty acid metabolic process
Ribonucleotide metabolic process
Ribose phosphate metabolic process
Carboxylic acid catabolic process
Monocarboxylic acid metabolic process
Lipid metabolic process
Organic substance catabolic process
Oxoacid metabolic process
Organic acid metabolic process
Cellular catabolic process
Catabolic process
Carboxylic acid metabolic process
Small molecule metabolic process
Oxidation-reduction process
Organic substance metabolic process
Cellular metabolic process
Metabolic process
Fold Enrichment
N. of Genes
-log10(FDR)
F.
Arginine biosynthetic process
Glutamine family amino acid biosynthetic process
Pyrimidine nucleobase metabolic process
Arginine metabolic process
Pyrimidine-containing compound metabolic process
Glutamine family amino acid metabolic process
Alpha-amino acid biosynthetic process
Cellular amino acid biosynthetic process
Alpha-amino acid metabolic process
Carboxylic acid biosynthetic process
Cellular amino acid metabolic process
Organonitrogen compound biosynthetic process
Organonitrogen compound metabolic process
Biosynthetic process
Cellular biosynthetic process
Organic substance biosynthetic process
Primary metabolic process
Nitrogen compound metabolic process
Organic substance metabolic process
Metabolic process
Fold Enrichment
N. of Genes
-log10(FDR)

A.

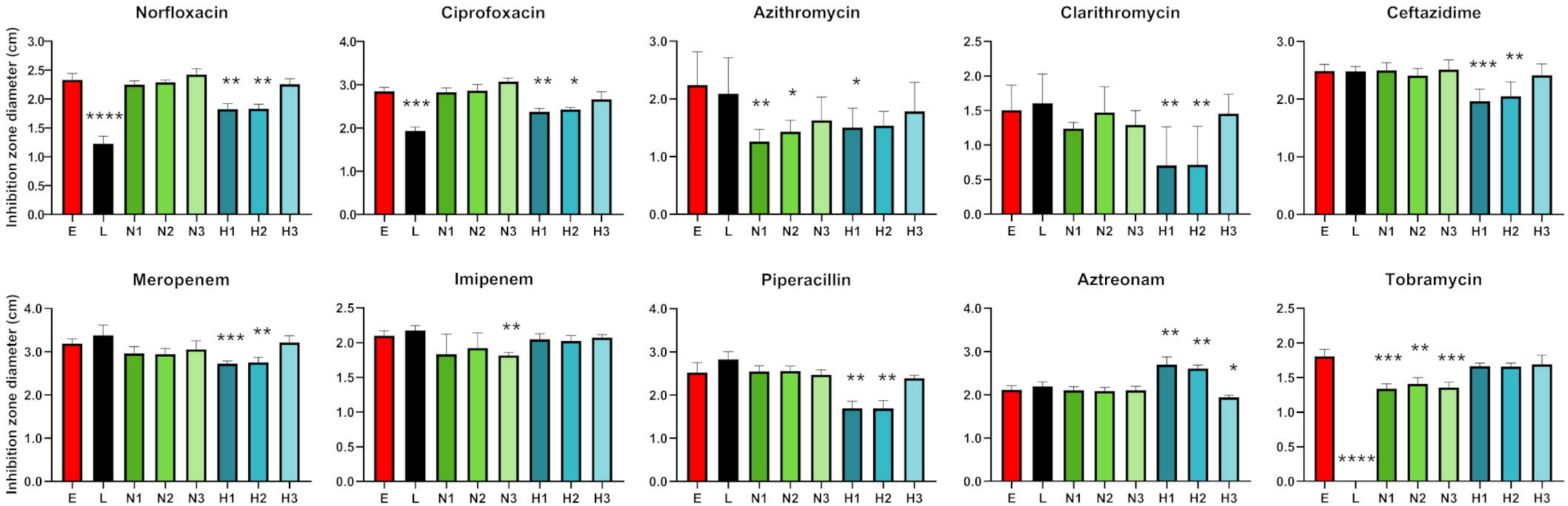

B.

Antibiotic	L	N1	N2	N3	H1	H2	H3	Antibiotic Class
Norfloxacin	↑	=	=	=	↑	↑	=	Fluoroquinolones
Ciprofoxacin	↑	=	=	=	↑	↑	=	
Azithromycin	=	↑	↑	=	↑	=	=	Macrolides
Clarithromycin	=	=	=	=	↑	↑	=	
Ceftazidime	=	=	=	=	↑	↑	=	Cephalosporins
Cefotaxime	=	=	=	=	=	=	=	
Meropenem	=	=	=	=	↑	↑	=	Carbapenems
Imipenem	=	=	=	↑	=	=	=	
Tobramycin	↑R	↑	↑	↑	=	=	=	Aminoglycosides
Piperacillin	↓	=	=	=	↑	↑	=	Penicillins
Aztreonam	=	=	=	=	↓	↓	↑	Monobactams
Tetracycline	= R	= R	= R	= R	= R	= R	= R	Tetracyclines

C.

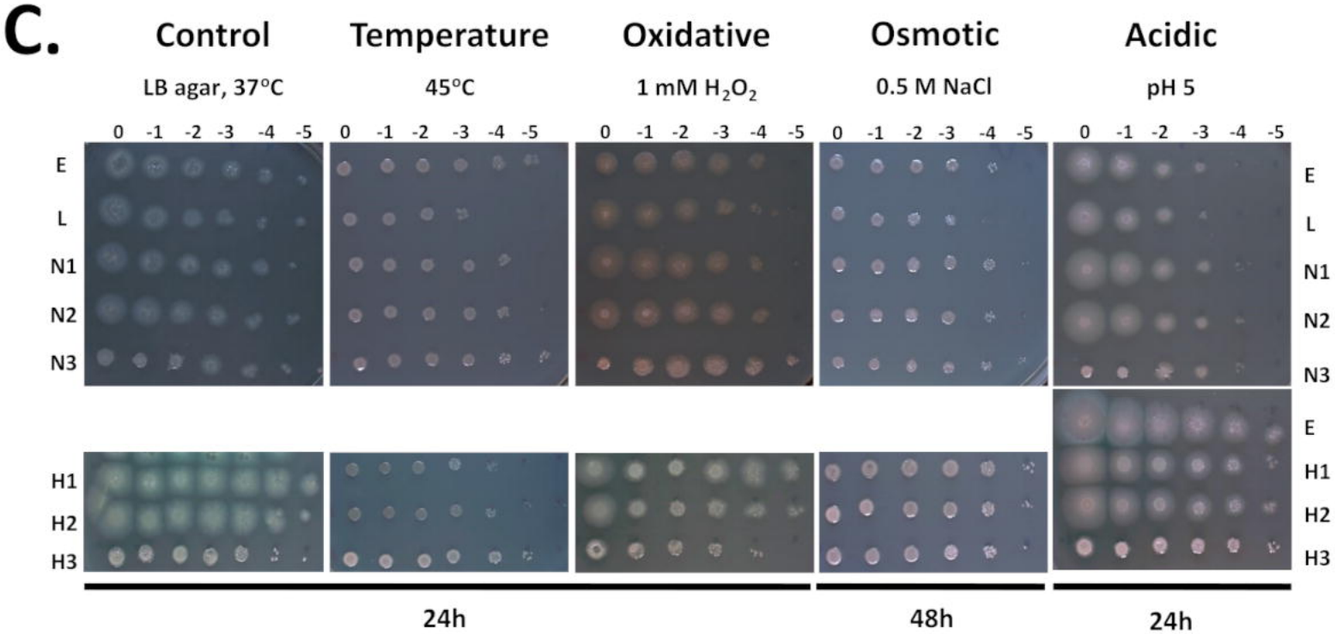

D.

Stress type	L	N1	N2	N3	H1	H2	H3
Temperature	↓	↓	↓	=	↓	↓	=
Osmotic	↓	↑	=	↑	↑	↑	↑
Oxidative	=	=	=	↑	↑	↑	=
Acidic	=	↑	↑	↑	=	=	=

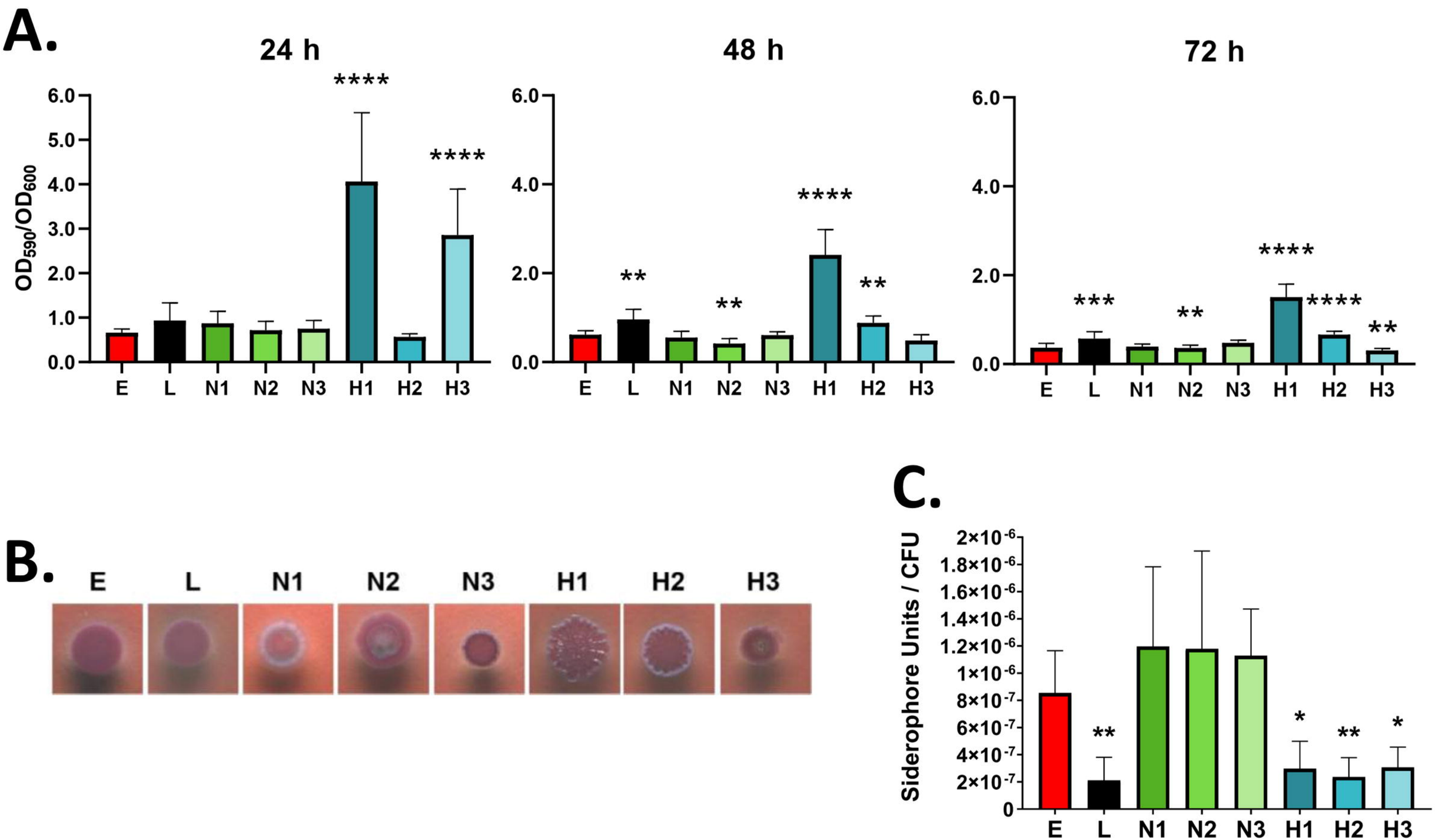
A.
24 h
48 h
72 h
OD590/OD600
6.0
5.0
4.0
3.0
2.0
1.0
0.0
****
**
***
E
L
N1
N2
N3
H1
H2
H3
B.
C.
Siderophore Units / CFU
2×10-6
1.8×10-6
1.6×10-6
1.4×10-6
1.2×10-6
1×10-6
8×10-7
6×10-7
4×10-7
2×10-7
0
*

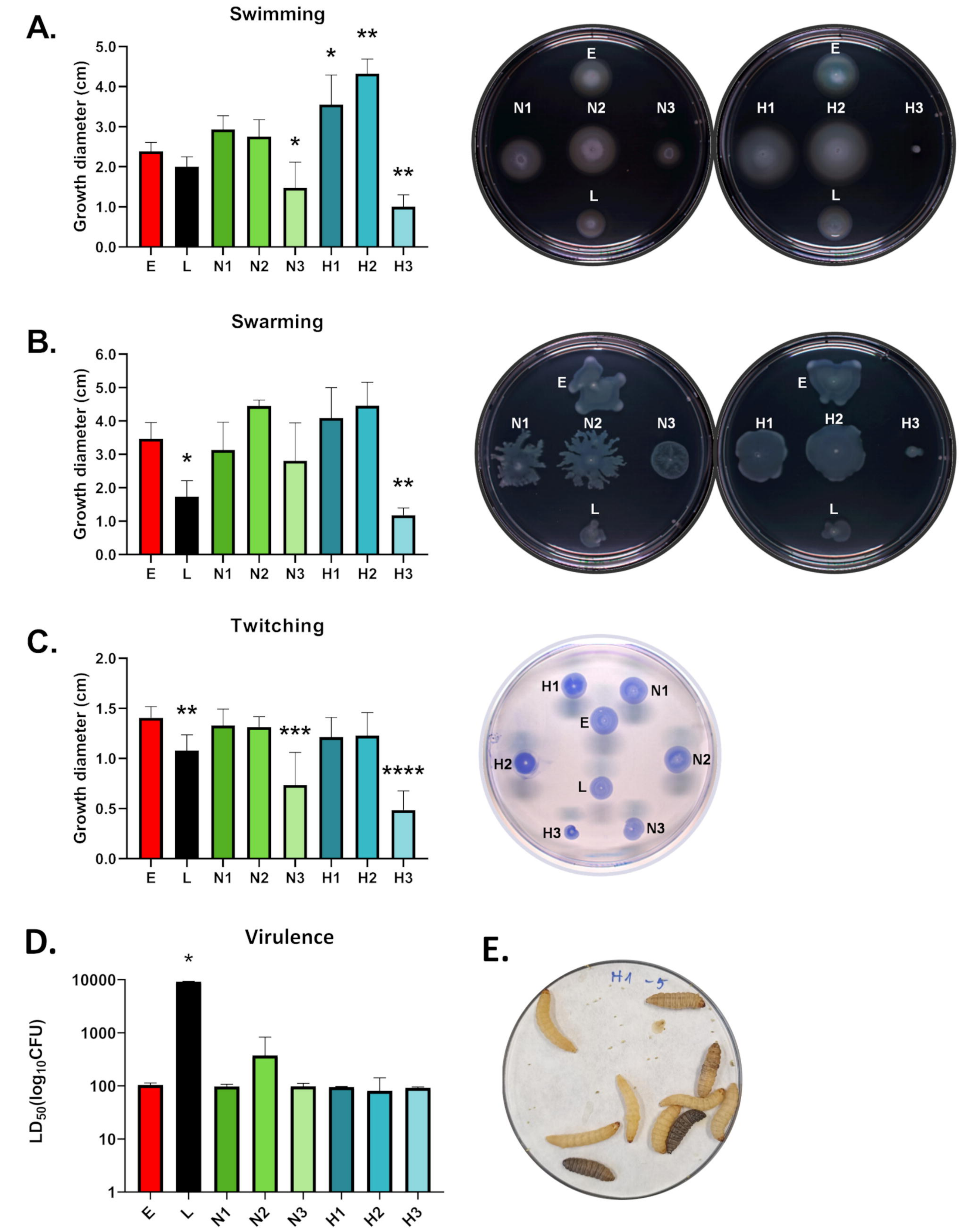
A.
Swimming
Growth diameter (cm)
5.0
4.0
3.0
2.0
1.0
0.0
*
**
*
**
E
L
N1
N2
N3
H1
H2
H3
B.
Swarming
Growth diameter (cm)
6.0
5.0
4.0
3.0
2.0
1.0
0.0
*
**
E
L
N1
N2
N3
H1
H2
H3
C.
Twitching
Growth diameter (cm)
2.0
1.5
1.0
0.5
0.0
**
***
****
E
L
N1
N2
N3
H1
H2
H3
D.
Virulence
LD50(log10CFU)
10000
1000
100
10
1
*
E
L
N1
N2
N3
H1
H2
H3
E.
H1 -5

Phenotype		L	N1	N2	N3	H1	H2	H3
SCVs (%)		58.0%	0.00	0.00	2.7%	76.9%	79.8%	0.7%
Pyocyanin		↓	↓	=	=	↓	↓	=
Antibiotic resistance		=	=	=	=	↑	↑	=
Stress resistance	Osmotic	↓	↑	=	↑	↑	↑	↑
	Oxidative	=	=	=	↑	↑	↑	=
	Heat	↓	↓	↓	=	↓	↓	=
	Acidic	=	↑	↑	↑	=	=	=
Biofilm 72h		↑	=	=	↑	↑	↑	=
Exopolysaccharide production		=	=	=	↑	↑	↑	=
Motility	Swimming	↓	↑	↑	↓	↑	↑	↓
	Swarming	↓	=	↑	↓	↑	↑	↓
	Twitching	↓	=	↑	=	=	↑	↓
Siderophore production		↓	=	=	=	↓	↓	↓
Virulence (*G. mellonella*)		↑	=	=	=	=	=	=

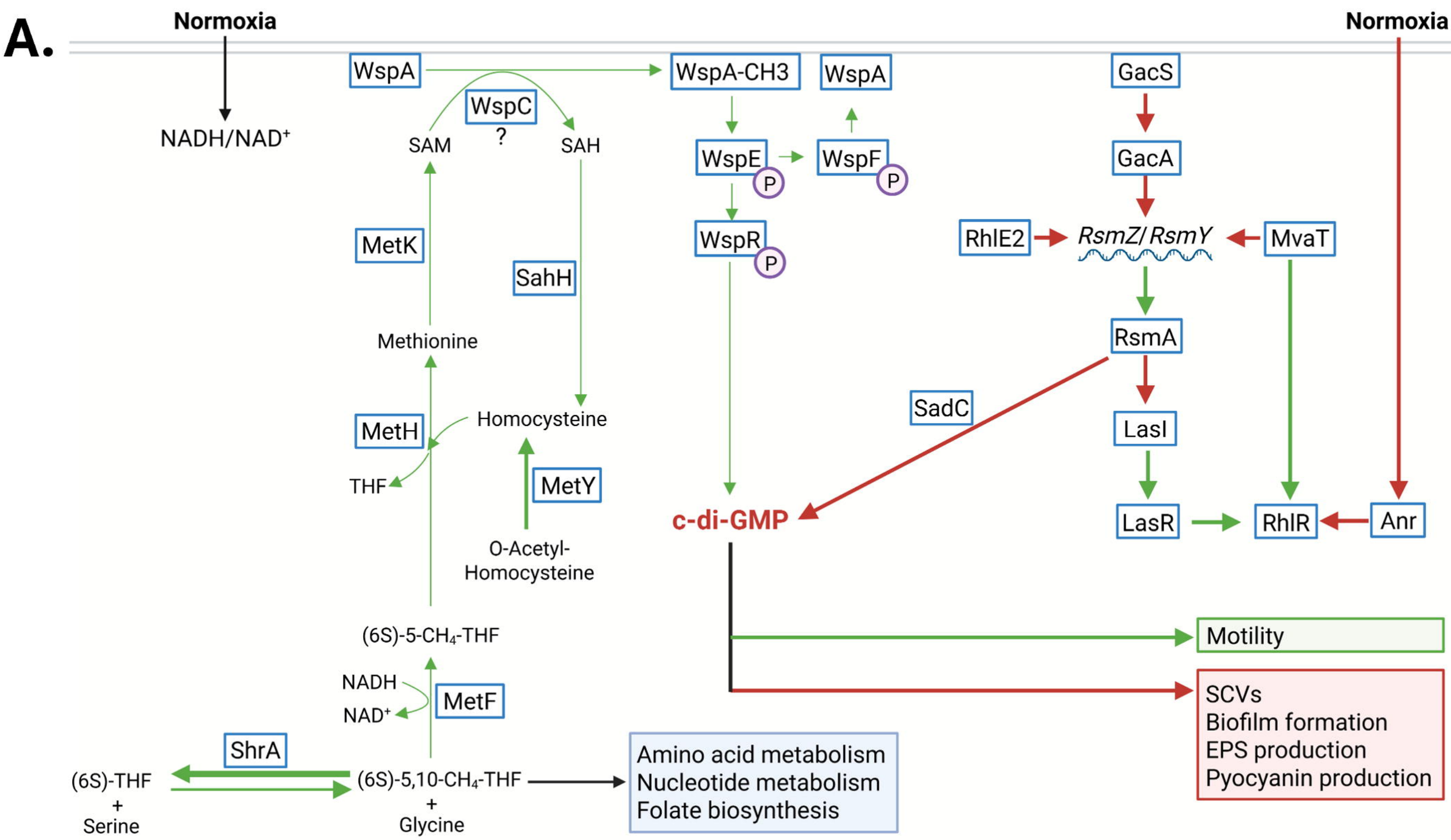
A.
Normoxia
NADH/NAD+
WspA
WspC
?
SAM
SAH
WspA-CH3
WspA
WspE
P
WspF
P
WspR
P
GacS
GacA
RhlE2
RsmZ/RsmY
MvaT
RsmA
SadC
LasI
LasR
RhlR
Anr
MetK
SahH
Methionine
MetH
Homocysteine
THF
MetY
O-Acetyl-
Homocysteine
c-di-GMP
Motility
(6S)-5-CH4-THF
NADH
NAD+
MetF
ShrA
(6S)-THF
+
Serine
(6S)-5,10-CH4-THF
+
Glycine
Amino acid metabolism
Nucleotide metabolism
Folate biosynthesis
SCVs
Biofilm formation
EPS production
Pyocyanin production

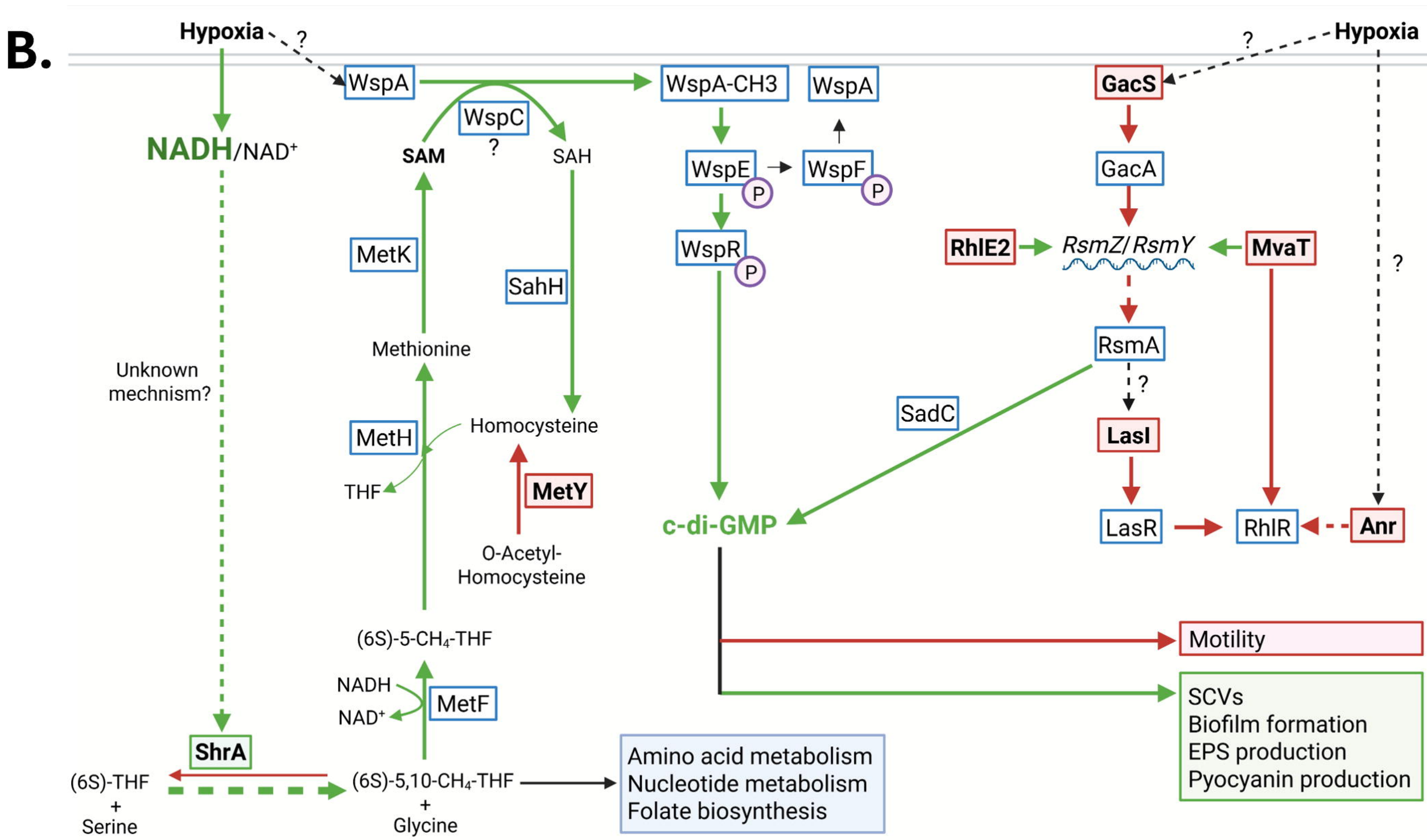
B.
Hypoxia
?
NADH/NAD+
WspA
WspC
?
SAM
SAH
WspA-CH3
WspA
WspE
P
WspF
P
WspR
P
GacS
GacA
RhlE2
RsmZ/RsmY
MvaT
RsmA
SadC
LasI
LasR
RhlR
Anr
MetK
SahH
Methionine
Unknown
mechnism?
MetH
Homocysteine
THF
MetY
O-Acetyl-
Homocysteine
c-di-GMP
Motility
(6S)-5-CH4-THF
NADH
NAD+
MetF
ShrA
(6S)-THF
+
Serine
(6S)-5,10-CH4-THF
+
Glycine
Amino acid metabolism
Nucleotide metabolism
Folate biosynthesis
SCVs
Biofilm formation
EPS production
Pyocyanin production